Biomass Burning in Amazonia: Emissions, Long-Range Transport of Smoke and Its Regional and Remote Impacts

K. M. Longo[1], S. R. Freitas[2], M. O. Andreae[3], R. Yokelson[4], and P. Artaxo[5]

Every year, biomass burning in Amazonia continues to release large amounts of trace gases and aerosol particles into the atmosphere. The consequent change from low to very high atmospheric concentrations of oxidants and aerosols therefore affects the radiative, cloud physical, and chemical properties of the atmosphere over Amazonia. This represents a dramatic perturbation to the regional climate, ecology, water cycle, and human activities. Given the magnitude of burning in Amazonia and the efficiency of the atmospheric transport processes of fire emissions, these perturbations can affect the climate system even on a global scale. This chapter summarizes the knowledge acquired in the ambit of the Large-Scale Biosphere-Atmosphere Experiment in Amazonia program about vegetation fire as a driving force of atmospheric disturbances over Amazonia. We describe the different fire behaviors for the region and present an updated review of emission and combustion factors for Amazonia. We discuss some of the available biomass-burning emission inventories for the Amazonian region, discussing their assets and limitations. We further discuss atmospheric transport processes that are the main drivers of the dispersion of fire emissions, introduce the most relevant concepts for numerical modeling of smoke transport, and show the general pattern of smoke transport over the South American continent. Finally, we present the current status of the understanding of local and remote impacts of smoke trace gases and aerosol particles, discussing the oxidizing power of the Amazonian atmosphere, as well as the radiation and heat budgets and consequences on cloud properties and distribution.

[1]Center for Space and Atmospheric Sciences, National Institute for Space Research, São José dos Campos, Brazil.

[2]Center for Weather Forecast and Climate Studies, National Institute for Space Research, Cachoeira Paulista, Brazil.

[3]Max Planck Institute, Mainz, Germany.

[4]Department of Chemistry, University of Montana, Missoula, Montana, USA.

[5]Institute of Physics, University of São Paulo, São Paulo, Brazil.

Amazonia and Global Change
Geophysical Monograph Series 186

10.1029/2008GM000847

1. INTRODUCTION: BIOMASS BURNING IN AMAZONIA

The composition of the atmosphere is controlled by several natural and anthropogenic processes, and emissions from biomass burning are one of its strongest drivers in the Southern Hemisphere [*Crutzen and Andreae*, 1990]. Agricultural residues have been burnt for millennia, and the reduction in forest area in North America and Europe over the last centuries has evidently contributed to the changes in atmospheric composition. More recently, during the last four to five decades, the rapid and intensive land use change in the tropics has led to more attention being paid to this issue.

It is important to emphasize that biomass burning as a major atmospheric driver is not only restricted to the tropics. The high concentration of aerosol particles and trace gases observed in the Amazonian and Central Brazilian atmosphere during the dry season is associated with intense anthropogenic biomass-burning activity. Ozone, carbon monoxide, nitrogen oxides, and aerosol particle concentrations over South America and the surrounding ocean areas are regulated by biomass-burning emissions from savannah and forest fires. About 9200 Teragram (dry weight) is burned annually [*Andreae and Merlet*, 2001; *Bergamaschi et al.*, 2000], contributing significantly to the atmospheric burden of pollutants. In South America, during the biomass-burning season, a regional smoke plume covering an area of about 4 to 5 million km^2 has been frequently observed through remote sensing of South America [*Prins et al.*, 1998]. Inhalable aerosol particles with concentration as high as 400 $\mu g\ m^{-3}$ have been measured close to the surface, and the column-integrated aerosol optical thickness reaches 4.0 to 5.0 (440 nm) over large areas of central Brazil [*Artaxo et al.*, 1998]. Ozone concentrations in excess of 100 ppb are frequently observed thousands of kilometers away from forest fires, and the ozone phytotoxicity certainly affects the unburned forest. On a regional and global scale, the persistent and heavy smoke layer over an extensive tropical region may alter the radiation balance and the hydrological cycling. Carbon uptake by the forest, expressed by the net ecosystem exchange (NEE) is heavily affected by the aerosol layer over the forest; where, at low aerosol levels, an increase of 30% to 40% in NEE was observed for aerosol optical depth (AOD) up to 1.2 at 550 nm [*Oliveira et al.*, 2007]. This effect happens because the aerosol particles in the atmosphere increase the diffuse solar radiation, and the forest canopy geometry leads to enhanced photosynthesis. But when the AOD exceeds about 1.5, the effect of the reduction in total solar flux starts to predominate, and NEE start to decrease; for values of AOD near 4 or 5, it shuts down almost completely. This effect of changing the ratio of diffuse to direct radiation has strong implication for the carbon balance over tropical forests [see *Artaxo et al*., this volume, and references therein].

A second strong effect of aerosol particles emitted through biomass burning is the resultant changes in cloud microphysics, development, and structure. Clouds are a critical ingredient of the radiation balance and the hydrological cycle. The presence of biomass-burning particles in the atmosphere also modifies the solar radiative balance by changing the cloud microphysics. These particles act as cloud condensation and ice nuclei, promoting changes in the cloud drop spectrum and, consequently, altering the cloud albedo and precipitation [*Rosenfeld et al.*, 2006]. This suggests that the biomass-burning effects may extrapolate the regional scale and influence the pattern of planetary redistribution of energy from the tropics to medium and high latitudes via convective transport processes. Changes in cloud cover due to the presence of large amounts of black carbon particles are well documented in the work of *Koren et al.* [2004, 2008] and *Kaufman and Koren* [2006]. See also *Artaxo et al*. [this volume] for an overview of this issue.

Emissions from the combustion of any type of fuel depend directly on the chemical composition of that fuel and the combustion conditions. For biomass burning, most data are available for wood combustion. Different tree species develop markedly different woody constituents during growth, and typically, all wood consists of various forms of lignin, celluloses, and fillers. Emission factors (EFs) are important because they are used in regional and global models to study the influence of the biomass-burning emissions on regional and global climate.

Deforestation in Brazilian Amazonia has been studied using remote sensing techniques [*Câmara et al.*, 2005; *Morton et al.*, 2005]. The average deforestation rate for the 1990s was 17,000 km^2 per year, increasing to approximately 25,000 km^2 in 2002 and 2003 [*Instituto Nacional de Pesquisas Espaciais* (*INPE*), 2008], going down to 10,000 km^2 in 2007 [see *Schroeder et al.*, this volume]. Up to 2005, an estimated area of 16% of the total Brazilian Amazonia, i.e., an area of 5.8 million km^2 was deforested [*INPE*, 2008]. Deforestation mainly occurs in the southern and eastern parts of Amazonia, while the central areas that are less accessible are relatively well preserved. Deforestation affects the ecosystem in several ways: First, there is a change in the energy and water balance when forest is replaced by pasture, and this change has the potential to alter the atmospheric water content and precipitation patterns [*Silva Dias et al.*, 2002]. Second, a large amount of aerosol particles is released into the atmosphere, as forests are cut and burned in the course of managing pastures and fields, leading to profound changes in the atmospheric composition [*Artaxo et al.*, 1998, 2002] and surface radiation balance [*Schafer et al.*, 2002a, 2002b; *Procópio et al.*, 2003, 2004]. Amazonia deforestation and biomass burning can trigger a positive feedback cycle of increased fire disturbance and local drought conditions, amplifying droughts linked to both anthropogenic global climate change and natural climate variability [*Nobre et al.*, 1991; *Marengo et al.*, 2008].

This chapter presents an overview of the knowledge acquired in the ambit of the Large-Scale Biosphere-Atmosphere Experiment in Amazonia (LBA) program about emissions to the atmosphere from vegetation fires in Amazonia. The atmospheric transport of smoke and their impacts on the atmospheric composition, weather, and climate at local, regional, and global scales will be addressed.

2. BIOMASS-BURNING EMISSION ESTIMATES

Biomass combustion is a complex mix of chemical and physical processes. A detailed description and references can be found in the work of *Yokelson et al.* [1996, 1997], which is summarized below.

The processes involved in biomass combustion can be visualized by considering the effects of increasing temperature on fresh biomass. The first effect of rising temperature is the distillation of absorbed species with low boiling points, mostly water. At higher temperatures (~500–700 K) bonds begin to break in the macromolecules that comprise biomass. This process is known as low-temperature pyrolysis, and it releases a white smoke and small molecules with sufficient vapor pressure to enter the gas phase. Most of the smoke particle species and gases are oxygenated organic compounds such as methanol and acetic acid. The selective release of oxygenated compounds leaves the remaining "parent" biomass enriched in carbon, a product known as "low-temperature char." At higher temperatures (700–900 K), the low-temperature char begins to emit aliphatic compounds (containing mostly C and H) further enriching the biomass in carbon and producing high-temperature char (high in aromatic components). The chemisorptions of O_2 on high-temperature char is exothermic, and it provides energy for gasification reactions that convert carbon in the solid char to products such as CO and CO_2. Intense gasification is commonly known as "glowing" combustion. A glowing front (typically 1000 K) can propagate across a fuel element pyrolyzing much or all of the biomass ahead of the front and producing a mix of all the products noted above [*Bertschi et al.*, 2003].

In the absence of flames, the particles and gases emitted by pyrolysis and glowing directly enter the atmosphere as pollutants. When the concentration of volatile gases and their temperature is above a threshold, they can react rapidly with oxygen to produce turbulent diffusion flames with temperatures typically near 1400 K. The flames efficiently oxidize the entrained volatile gases to species such as H_2O, CO_2, and NO_x. Incompletely oxidized species such as CO are also generated in comparatively small amounts. Black smoke that is high in elemental carbon is formed by condensation just above the flames. The flames are also important as a heat source to drive further pyrolysis of fresh biomass, which (along with glowing) generates more volatiles to feed continued flaming.

In practice, fires are usually ignited by applying sufficient heat to initiate flaming/glowing at a point. A mixture of flaming and glowing then propagates across the fuel bed and pyrolyzes much of the available fuel. During this time, most (but not all) of the pyrolysis and glowing products are oxidized by entrainment into the flames. Once the flames have passed across the whole fuel bed, the rate of volatile production and flaming begins to drop, along with the concentrations of most of the emitted species. At this point the probability of flame oxidation of the emitted volatiles also decreases, and the smoke begins to increasingly reflect the products of smoldering combustion. The flaming and mixed flaming/smoldering phases of the fire normally account for 50–95% of the total fuel consumption. A final smoldering-only phase continues as long as 5–10% of the heat generated by the fire is transferred to fresh fuel. The amount of fuel consumption by the smoldering phase is heavily dependent on fuel geometry with closely packed fuels being consumed much more efficiently [*Bertschi et al.*, 2003].

Ultimately, the biomass-burning emissions depend upon many controlling factors. In this section, we provide an updated review of the measured emission and combustion factors for Amazonia with an assessment of their accuracy and regional representativeness.

2.1. How Fire Behavior Affects Emission Measurements for Different Fire Types

Most anthropogenic fires in the tropics usually begin with ignition along one edge or two opposing edges of the treatment area. At the start of the fire, all the emissions are from flaming combustion and entrained in the flame-induced convection column. As the flame front propagates inward, the convection column also entrains the emissions from any smoldering combustion that continues in the area just vacated by the flames. In a homogeneous fuel bed, a steady mixture of flaming and smoldering emissions can be produced from much of the fuel. These emissions are best sampled from the air.

When smoldering continues after the convection envelope is too far away to entrain the emissions, or after convection from the entire site has ceased, the fire emissions are produced by what we define as residual smoldering combustion (RSC). RSC emissions must be sampled from the ground. Since flaming and smoldering combustion produce smoke with different chemical composition, the fire behavior described above is an important consideration for representative sampling of the emissions from different types of fires.

2.1.1. Major types of fires that occur in Brazilian Amazonia. Next is a brief summary of the fire types that are important in Brazilian Amazonia and relevant features for their associated emissions.

2.1.1.1. Savanna (Cerrado) fires. Part of the southern Amazon basin is covered by savanna [*Coutinho*, 1990] that is burned every 1–3 years to improve grazing. These fires rapidly

consume 5–10 t ha^{-1} of mostly grass [*Coutinho*, 1990; *Ward et al*., 1992; *Kauffman et al.*, 1994; *Andrade et al.*, 1999]. We expect that RSC normally accounts for <10% of fuel consumption [*Bertschi et al.*, 2003].

2.1.1.2. Primary deforestation fires. Evergreen tropical forest is the dominant ecosystem in the Amazon basin. Deforestation rates measured since 1978 have ranged from 11 to 29 × 10^3 km^2 a^{-1} (~2 × 10^6 ha annually (http://www.obt.inpe.br/prodes/)) [see also *Schroeder et al*., this volume]. Deforestation fires feature much greater total aboveground biomass (TAGB) loading than savanna fires: e.g., 288, 402, 265, 349 ± 21 (n = 7), and 292 t ha^{-1} reported by *Carvalho et al.* [1998, 2001], *Fearnside et al.* [1993], *Guild et al.* [1998], *and Ward et al.* [1992]. In these studies, the percentage of the TAGB consumed by the fire was 50, 21, 29, 48 (n = 7), and 53. RSC likely accounts for less than 10% of the total fuel consumption [*Christian et al.*, 2007].

2.1.1.3. Pasture maintenance fires. Pasture fires are intermediate in TAGB and fuel characteristics between savanna and primary deforestation fires because residual wood debris (RWD) from the first deforestation fire on the site usually persists for many years. Reported TAGB ranges from 119 t ha^{-1} (with 87% of TAGB being RWD in a 4-year-old pasture) to 53 t ha^{-1} (47% RWD, in a 20-year-old pasture) [*Barbosa and Fearnside*, 1996; *Guild et al.*, 1998; *Kauffman et al.*, 1998]. Large-diameter RWD that burned mostly by RSC was reported to account for 38–49% of the fuel consumption in the above studies. *Fearnside* [1990] reported that ~75% of the burned forest was converted to pasture. Pastures are usually subjected to maintenance burns every 2–3 years for 10–20 years [*Guild et al*., 1998] before they are abandoned or converted to other uses. As a result, pastures occupy most of the deforested land, and pasture burning is the most common type of fire in Amazonia on an area basis. For Brazilian Amazonia, the total biomass burned in pasture fires is comparable to the total burned in deforestation fires: ~240 Tg a^{-1} each [*Kauffman et al.*, 1998].

2.1.2. Recent land use trends affecting fire emissions. In Brazil, the above picture is now being modified by the rapid growth in large-scale, mechanized soybean and sugar cane production, especially in the state of Mato Grosso. The croplands for soy are provided both by conversion of pastures and direct conversion of primary or secondary forest. To enable mechanized agriculture, all the large-diameter wood must be removed, which is only practical using fire, often assisted by mechanical piling of the fuel. This could imply larger fuel loadings and larger, more intense fires. *Morton et al*. [2006] found that within Mato Grosso from 2001 to 2004, pasture was still the main use following deforestation, but that fraction was decreasing (to 66%), and direct transition to large (>25 ha) areas of cropland accounted for up to 23% of deforestation. Deforestation for cropland accounted for 28% of clearings larger than 200 ha in 2003. We speculate that the expansion of mechanized agriculture may be associated with a regional increase in the area of individual fires, the fuel consumption per unit area, and fire intensity.

2.2. Biomass-Burning Emissions Measurements Relevant to Amazonia

In 1979 and 1980, *Crutzen* [1995] made the first airborne measurements of CO, CH_4, total nonmethane hydrocarbons, and other species emitted by Amazonian fires. A ground-based component speciated selected nonmethane organic compound (NMOC) emissions [*Greenberg et al*., 1984]. As part of the Atmospheric Boundary Layer Experiment (ABLE 2A) in 1985, *Andreae et al*. [1988] added emissions measurements for CO_2, CO, NO_x, SO_2, and major particle constituents and also characterized some postemission transformations. In 1990, *Ward et al*. [1992] made tower-based measurements that closely related the EFs for the main trace gases and $PM_{2.5}$ to vegetation type as part of the Biomass Burning Airborne and Spaceborne Brazil experiment. *Blake et al*. [1996] speciated additional selected hydrocarbons in slightly aged biomass burning plumes in 1992. In 1995, the most complete biomass-burning experiment up to that time was carried out in Amazonia: Smoke, Clouds, and Radiation-Brazil [*Kaufman et al*., 1998]. *Ferek et al*. [1998] reported detailed measurements of both the trace gas and particle species and particle optical properties. The data from all the above campaigns was synthesized in a review paper by *Andreae and Merlet* [2001]. They recommended EFs (grams of compound emitted per kilogram of dry fuel burned) for the main global fire types based on data available at the time.

The above work include only a small amount of data for oxygenated volatile organic compounds (OVOC), which are difficult to measure, yet critical in tropospheric chemistry [*Trentmann et al*., 2005], accounting for ~80% of the NMOC emitted by fires [*Yokelson et al*., 2008]. In 2000 and 2001, field and laboratory measurements of savanna fire emissions were made for the first time with instrumentation capable of quantifying both hydrocarbons and OVOC [*Yokelson et al*., 2003; *Christian et al*., 2003]. Thus, to estimate the emissions from Amazonian savanna fires, an up-to-date source is the table for savanna fires in the work of *Christian et al*. [2003] with *Andreae and Merlet* [2001] for additional species. The EF can be adjusted for RSC by referring to *Bertschi et al*. [2003] and *Christian et al*. [2007].

In the 2002 Amazonian dry season, the Smoke, Aerosol, Clouds, Rainfall, and Climate Campaign (SMOCC) detailed the chemistry and physics of the biomass-burning particles and their interaction with clouds [*Chand et al*., 2006; *Rissler et al*., 2006; *Vestin et al*., 2007; *Fuzzi et al*., 2007]. The number of particles emitted per unit amount of biomass burned was quantified to improve assessments of the affects on cloud physics [*Guyon et al*., 2005].

During the 2004 dry season, the Tropical Forest and Fire Emissions Experiment (TROFFEE) took place in Brazilian Amazonia as part of LBA. There were two major fire-related goals in TROFFEE. One was to employ both airborne sampling of lofted plumes and ground-based sampling of RSC so that improved fire-integrated EF could be estimated for both the main fire types: deforestation and pasture maintenance fires [*Yokelson et al*., 2007; *Christian et al*., 2007]. The second objective was to employ instrumentation capable of measuring all the major types of organic emissions [*Karl et al*., 2007]. Nineteen fires were sampled from the air, and five were sampled from the ground. The results were synthesized as described by *Yokelson et al*. [2008] to produce recommended EF for the two main fire types in Brazilian Amazonia (Table 1).

2.3. Natural Variation in Emission Factors

In Figure 1, we plot the fire-average EF for selected compounds versus modified combustion efficiency (MCE = $\Delta CO_2/(\Delta CO_2 + \Delta CO)$, which serves as an indicator of the relative amount of flaming and smoldering combustion for biomass burning. This shows the natural variation in EF resulting from deforestation fires burning under a range of vegetative/environmental conditions and different mixtures of flaming and smoldering combustion. Figure 1a shows the NO_x EF, which increased as MCE (and thus flaming combustion) increased. Figures 1b–1d shows the pattern typical for NMOC, the EF for these "smoldering compounds" increased with decreasing MCE. Figure 1e shows that $EFPM_{10}$ also increased with decreasing MCE. The range in EF (with MCE) for the data shown is about a factor of two.

In theory, capturing the variation in EF with MCE would significantly enhance the accuracy of emission estimates and the input for local-global models. For instance, if we include the RSC measurements of *Christian et al*. [2007], the $EFCH_4$ varies by about a factor of 20 over the MCE range sampled during TROFFEE. Unfortunately, it is not possible to measure the MCE of fires from space as they occur. One cannot even be confident of seasonal trends in average MCE for fires in the major, global biomass-burning areas for reasons discussed in the work of *Yokelson et al*. [2007]. For example, in TROFFEE, there was evidence that the MCE of lofted plumes increased as the dry season progressed, but it is suspected that the amount of low-MCE RSC may also increase as the large diameter fuels dry out [*Yokelson et al*., 2007]. Thus, for now, one MCE and a set of associated EF for all the detected emissions was estimated that are intended for application to the whole dry season in Table 1. The EF in Table 1 represents only fresh, minutes-old smoke. This is because shortly after emission, large, rapid changes in trace gas and particle chemistry and particle mass can occur as documented elsewhere [*Hobbs et al*., 2003; *Yokelson et al*., 2007, 2009].

2.4. Higher Particle Emission Factors Measured During TROFFEE

The average particle EFs measured during TROFFEE are significantly larger than in previous work or recommendations. *Ferek et al*. [1998] reported a range of $EFPM_4$ from 2 to 21 g kg^{-1} and a study average of ~11 g kg^{-1} for Brazilian deforestation fires. The tower-based measurements of *Ward et al*. [1992] returned values for $EFPM_{2.5}$ ranging from 6.8 to 10.4 g kg^{-1} with an average of ~9 g kg^{-1} for forest fuels. The TROFFEE average value for PM_{10} is significantly higher at 17.8 ± 4.1 g kg^{-1}. For most types of biomass burning, the PM_{10} values are about 20% higher than the $PM_{2.5}$ or PM_4 values [*Artaxo et al*., 1998]. Applying this factor to the study average of *Ferek et al.* [1998] gives a projected PM_{10} of ~13 g kg^{-1}, lower than the TROFFEE average, but within the uncertainty. One reason why the TROFFEE $EFPM_{10}$ is higher than the projected $EFPM_{10}$ based on *Ferek et al.* [1998] could be related to fire size and intensity. *Ferek et al.* [1998] noted that their largest and most intense fire in Brazil had a much higher $EFPM_4$ or PM_4/CO ratio than the other Brazilian fires they sampled. They proposed that EFPM increases with fire size and intensity and cited $EFPM_{3.5}$ measurements from 15 to 25 g kg^{-1} (implying an average PM_{10} of ~25 g kg^{-1}) for large, intense North American fires [*Radke et al*., 1991; *Hobbs et al.*, 1997]. In the TROFFEE data, the lowest $EFPM_{10}$ (12–14 g kg^{-1}) are from the smallest fires sampled [*Yokelson et al*., 2007]. The largest $EFPM_{10}$ (26.4 g kg^{-1}) was obtained on the largest and most intense plume encountered. Thus, we speculate that the larger TROFFEE EFPM for Brazil could be due to sampling larger, more-intense fires (on average) than in previous studies in Brazil. If correct, this suggests two topics deserving further research: (1) what size and intensity of fires contribute to what fraction of the regional biomass burning, and (2) is there a trend in fire size related to trends in land-use (discussed in section 2.1.1).

2.5. Regional Biomass-Burning Emissions Inventories for South America

Bottom-up, biomass-burning emission inventories are essentially the product of the amount of biomass burned times

Table 1. Emission Factors (EF) for Primary Tropical Deforestation and Pasture Maintenance Fires

				Recommended EF		Annual Averages	
Species (Tropical Forest and Fire Emissions Experiment (TROFFEE) data)	Ground Average[a] ($g\ kg^{-1}$)	Air Average[b] ($g\ kg^{-1}$)	Lab Average[c] ($g\ kg^{-1}$)	Primary Deforestation Method[d] ($g\ kg^{-1}$)	Pasture Maintenance Method[e] ($g\ kg^{-1}$)	Amazon Region[f] (Tg)	Global Tropical Deforestation[g] (Tg)
CO_2	1343	1615	1677	1601	1506	746	2130
CO	228.8	101.4	57.5	107.8	152.4	62.4	143.4
Modified combustion efficiency	0.788	0.910	0.949	0.904	0.861		
NO_x as NO	0.33	1.77	1.67	1.70	1.19	0.69	2.25
CH_4	17.12	5.68	3.82	6.25	10.26	3.96	8.32
C_2H_4	1.42	0.95	1.83	0.98	1.14	0.51	1.30
C_2H_2	0.09	0.28	0.33	0.27	0.20	0.11	0.36
C_3H_6	1.43	0.45	0.56	0.50	0.84	0.32	0.66
HCOOH	0.26	0.59	0.58	0.57	0.46	0.25	0.76
CH_3COOH	19.73	3.43	2.84	4.25	9.95	3.41	5.65
HCHO	1.88	1.66	0.66	1.67	1.75	0.82	2.23
CH_3OH	10.30	2.57	2.29	2.95	5.66	2.07	3.93
Phenol	2.42	0.34	0.81	0.45	1.17	0.39	0.60
Acetol + methyl acetate	8.89	0.72	1.81	1.13	3.99	1.23	1.50
Furan	2.08	0.33	0.45	0.41	1.03	0.35	0.55
NH_3	1.64	1.08	3.39	1.10	1.30	0.58	1.47
HCN	0.35	0.68	0.39	0.66	0.54	0.29	0.88
Species with no ground data				Method[h]	Method[i]		
C_2H_6		0.90		1.01	1.80	0.67	1.34
Acetonitrile		0.37	0.5	0.41	0.74	0.28	0.55
Acetaldehyde		1.38	1.71	1.55	2.77	1.04	2.06
Acrylonitrile		0.04	0.29	0.04	0.08	0.03	0.06
Acrolein		0.58	1.34	0.65	1.16	0.43	0.86
Acetone		0.57	0.99	0.63	1.13	0.42	0.84
Propanal		0.09	0.16	0.10	0.18	0.07	0.13
Pyrrole		0.11	0.42	0.12	0.22	0.08	0.17
Isoprene		0.37	0.46	0.42	0.75	0.28	0.56
Methyl vinyl ketone		0.35	0.46	0.39	0.70	0.26	0.52
Methacrolein		0.14	0.18	0.15	0.28	0.10	0.21
Crotonaldehyde		0.21	0.28	0.24	0.42	0.16	0.31
Methyl ethyl ketone		0.45	0.78	0.50	0.90	0.34	0.67
Methyl propanal		0.16	0.28	0.18	0.32	0.12	0.24
Benzene		0.26	0.65	0.30	0.53	0.20	0.39
C6 Carbonyls		0.21	0.61	0.24	0.42	0.16	0.32
3-Methylfuran		0.53	0.77	0.59	1.05	0.39	0.79
2-Methylfuran		0.08	0.11	0.08	0.15	0.06	0.11
Hexanal		0.01		0.01	0.03	0.01	0.02
2,3-Butanedione		0.66	1.29	0.73	1.31	0.49	0.98
2-Pentanone		0.07	0.14	0.08	0.14	0.05	0.10
3-Pentanone		0.03	0.06	0.03	0.06	0.02	0.05
Toluene		0.20	0.56	0.22	0.39	0.15	0.29
Other substituted furans		1.08	1.55	1.21	2.17	0.81	1.61
Furaldehydes		0.26	0.41	0.29	0.51	0.19	0.38
Xylenes		0.13	0.34	0.14	0.26	0.10	0.19
Ethylbenzene		0.08	0.18	0.08	0.15	0.06	0.11

Table 1. (continued)

Species (Tropical Forest and Fire Emissions Experiment (TROFFEE) data)	Ground Average[a] ($g\ kg^{-1}$)	Air Average[b] ($g\ kg^{-1}$)	Lab Average[c] ($g\ kg^{-1}$)	Recommended EF: Primary Deforestation Method[d] ($g\ kg^{-1}$)	Recommended EF: Pasture Maintenance Method[e] ($g\ kg^{-1}$)	Annual Averages: Amazon Region[f] (Tg)	Annual Averages: Global Tropical Deforestation[g] (Tg)
Other TROFFEE species[j]							
PM_{10}		17.83		18.5	23.4	10.06	24.61
$PM_{2.5}$			9.93	14.8	18.7	8.04	19.68
Glycolaldehyde			0.87	1.32	3.09	1.06	1.75
Propanenitrile			0.61	0.09	0.17	0.06	0.12
OCS[k]		0.0247				0.0119	0.0329
DMS[k]		0.0022				0.0011	0.0030
CFC 12[k]		0.0028				0.0014	0.0037
$MeONO_2$[k]		0.0163				0.0078	0.0217
$EtONO_2$[k]		0.0057				0.0027	0.0076
i-$PrONO_2$[k]		0.0010				0.0005	0.0013
n-$PrONO_2$[k]		0.0003				0.0002	0.0005
2-$BuONO_2$[k]		0.0006				0.0003	0.0008
1-Butene[k]		0.0200				0.0096	0.0266
Trans-2-Butene[k]		0.0161				0.0077	0.0214
Cis-2-Butene[k]		0.0202				0.0097	0.0268
Total identified nonmethane organic compound				25.77	48.70	17.87	34.28
Other major species[l]							
H_2				3.8		1.82	5.05
N_2				3.1		1.49	4.12
SO_2				0.57		0.27	0.76

[a]From *Christian et al.* [2007].
[b]From *Yokelson et al.* [2007].
[c]Average of Fourier transform infrared spectrometers and proton transfer reaction–mass spectrometers if measured by both.
[d]Assuming 5% of ground average and 95% of airborne average [*Christian et al.*, 2007].
[e]Assuming 40% of ground average and 60% of airborne average [*Christian et al.*, 2007].
[f]Assuming 240 Tg biomass burned in each fire type [*Yokelson et al.*, 2007].
[g]Assuming 1330 Tg biomass burned [*Andreae and Merlet*, 2001] coupled with TROFFEE primary deforestation EFs.
[h]Computed from 1.12 times air average [*Yokelson et al.*, 2008].
[i]Computed from 2.00 times air average [*Yokelson et al.*, 2008].
[j]See *Yokelson et al.* [2008] for computation method.
[k]Based on one canister sample of smoke from *Yokelson et al.* [2007].
[l]From *Andreae and Merlet* [2001].

an EF. The estimation of the biomass burned can be accomplished if the aboveground biomass density, the combustion factor (the fraction of the fuel load actually combusted), and the burned area are available. In the late 1970s, *Hao and Liu* [1994] built a database for the spatial (5°) monthly distribution of the amount of biomass burned in tropical America, described in a paper which also includes estimates for African and Asian continents. The biomass-burning inventory that is commonly used by global models, part of the global emission source database called Emission Database for Global Atmospheric Research (EDGAR) [*Olivier et al.*, 1999], with 2.5° resolution and monthly time variation, is based on the work of *Hao and Liu* [1994]. *Duncan et al.* [2003] (hereafter D2003) combined fire-count data from the Along Track Scanning Radiometer and the advanced very high resolution radiometer (AVHRR) World Fire Atlases to determine the typical seasonal and interannual variability of biomass-burning emissions with a $1^\circ \times 1^\circ$ spatial resolution. Using the Total Ozone Mapping Spectrometer Aerosol Index as a proxy to estimate the strength of emissions, the authors estimated the mean variability of CO emissions from biomass burning. More recently, *Giglio et al.* [2006] and *Van der Werf et al.*

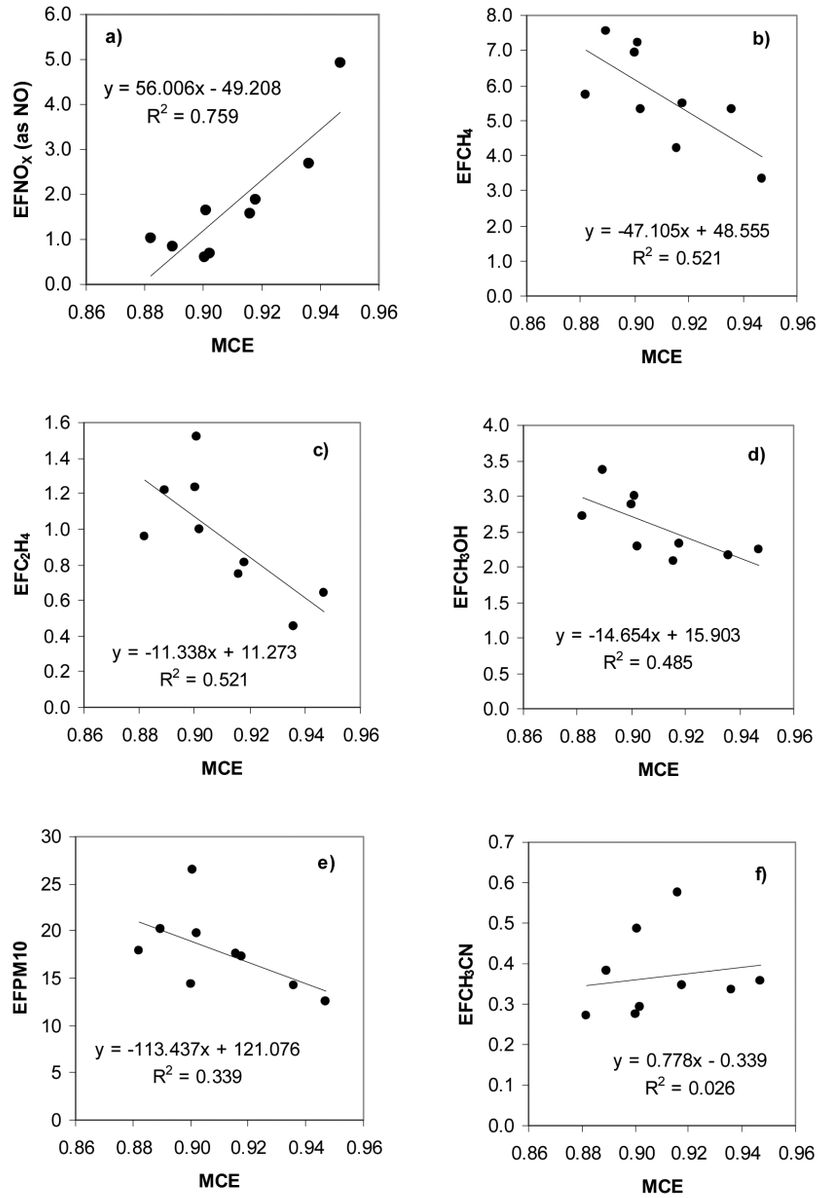

Figure 1. Fire-average emission factors (EF) plotted versus fire-average modified combustion efficiency for selected compounds [*Yokelson et al.*, 2007]: (a) NO_x, (b) CH_4, (c) EFC_2H_4, (d) $EFCH_3OH$, (e) PM_{10}, and (f) CH_3CN. The range of EF shows that significant variability is an inherent feature of biomass burning.

[2006] using burned area estimates from remote sensing, a biogeochemical model, and EFs from the literature, estimated fire emissions during the 8-year period from 1997 to 2004. This dataset, called Global Fire Emissions Database (GFED), has $1^\circ \times 1^\circ$ spatial resolution with 8-day and 1-month time steps. The Global Wildland Fire Emission Model (GWEM) provides emissions for several species based on the data from the European Space Agency's monthly Global Burnt Scar satellite product (GLOBSCAR) and more recently GBA2000 of the Joint Research Centre of the European Commission

and results from the Lund-Potsdam-Jena Dynamic-global vegetation model for the year 2000. GWEM yields over five times less carbon monoxide emissions than GFED estimation for South America and presents an early maximum emission in August, against the agreement of a maximum in September of all the inventories cited above. The relatively poor result of GWEM for South America was attributed mainly to the insufficient performance of the global burnt area products GLOBSCAR [*Hoelzemann et al.*, 2004] and GBA2000 [*Hoelzemann*, 2007] over this region.

As a result of an effort motivated by the necessity of biomass-burning emission estimates with daily resolution for operational chemical weather forecasting over the South American (SA) continent, the Brazilian Biomass Burning Emission Model (BBBEM) uses a daily hybrid remote sensing fire product in order to minimize missing remote sensing fire observations [*Freitas et al.*, 2005; *Longo et al.*, 2007]. The fire database presently utilized is a combination of the Geostationary Operational Environmental Satellite (GOES)-Wildfire Automated-Biomass Burning Algorithm product [*Prins et al.*, 1998], the Brazilian National Institute for Space Research fire product, which is based on the AVHRR aboard the NOAA polar orbiting satellites series [*Setzer and Pereira*, 1991; *Setzer and Malingreau*, 1996], and the Moderate Resolution Imaging Spectroradiometer (MODIS). The most recent GWEM version (1.4) including a correction for South America based on BBBEM methodology enhanced estimated CO emissions by 30% and improved the seasonality, shifting the emission maximum to September [*Hoelzemann*, 2007].

An intercomparison between the four inventories described above for CO from vegetation fires in South America was carried out by *Longo et al.* [2007]. The 3-monthly mean (August, September, and October 2002) of CO flux (mg m^{-2} day^{-1}) is shown in Plate 1, according to (a) BBBEM, (b) GFED, (c) D2003, and (d) EDGAR. D2003 refers to the mean seasonal estimation with 1° resolution. For GFED, the 1° and 8-day time resolution data corresponding to the above mentioned time period were used. The inventories BBBEM, GFED, and that of D2003 show general agreement with respect to the emission locations and have strong gradient of the emission field. On the other hand, EDGAR prescribes a too wide and smooth emission field with values less than 150 mg m^{-2} day^{-1}. BBBEM shows general agreement with the GFED in terms of patterns and estimation. D2003 shows also similar location patterns; however, over central Brazil and Mato Grosso state (from 20°S to 12°S and from 60°W to 40°W) the emissions are much higher than BBBEM and GFED. The inventories all show the maximum emission over the so-called arc of deforestation [see *Schroeder et al*., this volume], as expected. From all the three inventories, BBBEM yields the finest scale, since its spatial resolution can be as fine as the pixel size of the satellite sensor used for fire detection. Also, as it is based on fire count detection, BBBEM emissions are very well correlated with the number of detected fires within South America, but they are not directly proportional due to the different biomes and associated EFs attributed to each fire location. GFED and BBBEM are comparable during August, but GFED becomes much lower in September; this behavior is unexpected, since this month corresponds to the peak of the burning season. In October, fires started to be inhibited by rainfall and presented a sharp reduction in number during the last week. In this case, BBBEM, GFED, and D2003 showed the expected decrease, while EDGAR prescribed a small increase for October. It is worth noting that, because of its finest spatial and temporal resolution, BBBEM is able to prescribe emissions only where and when fires were in fact detected, an important feature for regional chemical weather forecasting [*Longo et al.*, 2007].

However, all these inventories are undeniably highly sensitive to the limitations and inherent uncertainties of the EFs and input data sets used for biomass-burned estimates. Newer and promising methodologies use the fire radiative energy to estimate emission rates [*Kaufman et al.*, 2003; *Riggan et al.*, 2004; *Ichoku and Kaufman*, 2005; *Smith and Wooster*, 2005; *Pereira*, 2008]. Also, recent studies have been showing the importance of improving spatial and temporal resolution of emission inventories for regional and even global modeling purposes. Regarding EFs, the addition of many reactive OVOC compounds to the list of quantified species emission (section 2.2) represents a valuable piece of information for atmospheric chemistry modelers. Incorporating the TROFFEE EF for RSC into bottom-up estimates of fire emissions from Amazonia increases the estimated annual regional fire emissions for several important VOC within the range of 10–50%. Photochemical box models show that one important effect of increased VOC is to speed up the initial smoke photochemistry [*Mason et al*., 2001, 2006; *Trentmann et al*., 2005]. Higher VOC emissions also imply greater potential for secondary aerosol formation [*Yokelson et al*., 2008, 2009].

3. LONG-RANGE TRANSPORT OF BIOMASS-BURNING PRODUCTS IN AMAZONIA

Atmospheric transport is driven mainly by the wind speed at the large scale and turbulence at the local scale. The typical transport time scales for atmospheric constituents are 1–2 years for interhemispheric exchange, 2 weeks for meridional transport throughout latitude belts, and about a month for the vertical transport in the troposphere [*Kley*, 1997]. However, the atmospheric transport of biomass-burning emissions over tropical regions is strongly associated both with the typical intense deep moist convection and the potent updrafts

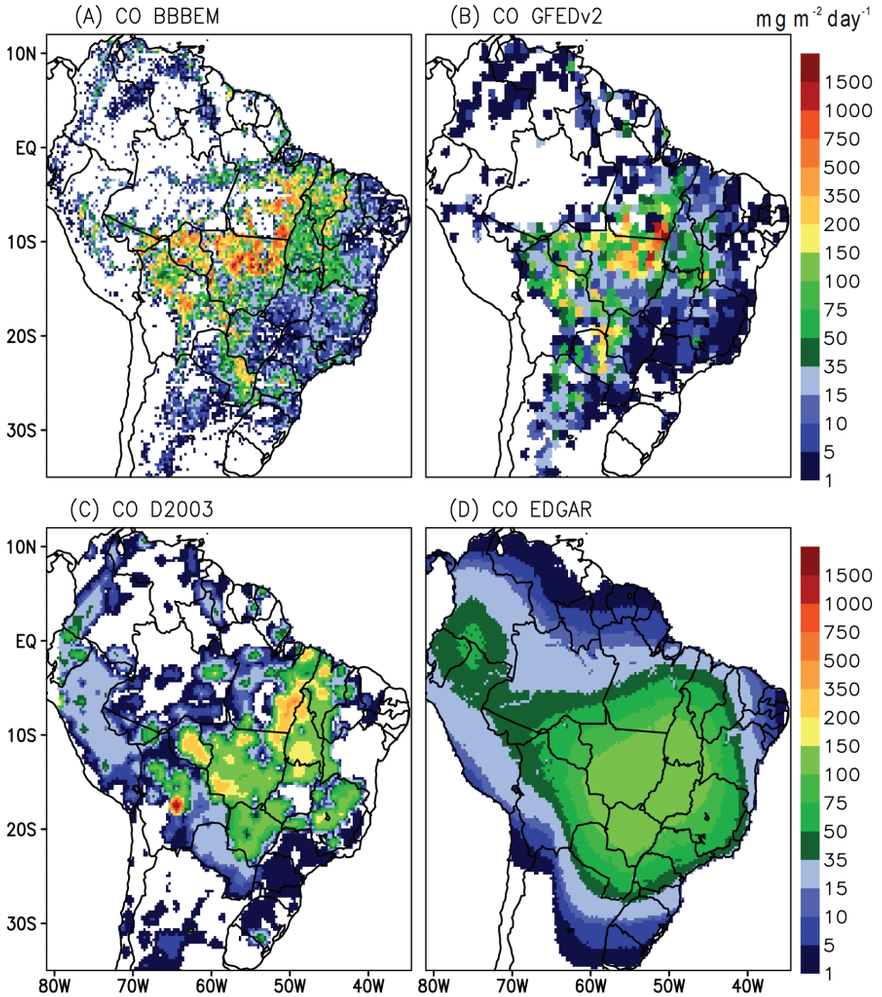

Plate 1. The 3-monthly mean CO distribution of four biomass-burning inventories (a) Brazilian Biomass Burning Emission Model, (b) Global Fire Emissions Database, (c) *Duncan et al.* [2003], and (d) Emission Database for Global Atmospheric Research for August–November 2002 [*Longo et al.*, 2007]. The color scale refers to the mean amount of CO emitted in mg m^{-2} day^{-1}.

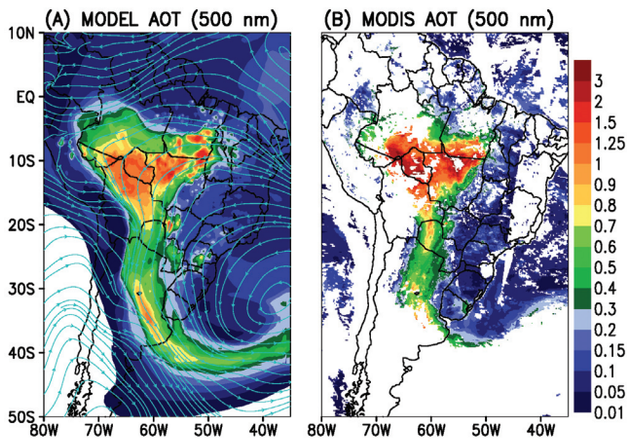

Plate 2. Aerosol optical depth at 500 nm (color scale) for 27 September 2002 from (a) CCATT-BRAMS model and (b) Moderate Resolution Imaging Spectroradiometer retrieval. The streamlines at 2 km height from the model are also shown in Plate 2a.

related with the initial buoyancy provided by vegetation fires. These very efficient mechanisms of vertical transport tend to boost the large-scale atmospheric transport and significantly reduce the global mixing time of biomass-burning emissions. This is related to higher wind speeds in the free troposphere, where the pollutants are more rapidly advected away from the source regions. Also, when the pollutants are transported to the free troposphere, their residence time increases because removal processes are much less efficient than in the planetary boundary layer (PBL). These processes altogether define the vegetation fires that are widely spread over tropical regions as a key agent on the regional and global distribution of trace gases and aerosol particles and their consequent impacts on regional and global climate.

3.1. Numerical Modeling of the Atmospheric Transport of Biomass-Burning Emissions

Numerical modeling of atmospheric biomass-burning emission transport requires the solution of the continuity equation for trace gases and aerosol particles mixing ratios $s_\eta = \rho_\eta/\rho_0$:

$$\frac{\partial s_\eta}{\partial t} + \vec{v}.\Delta(s_\eta) = \frac{Q_\eta}{\rho_0}, \tag{1}$$

where ρ_η and ρ_0 are the densities of the tracer η and the air, respectively, and $\vec{v}$ is the wind velocity. The term Q_η, normally called forcing, contains all the physical and chemical processes for production and loss of the species, η, which are mainly emissions (already described in section 2 for the biomass-burning sources), chemical reactions, particle transformations, or dry and wet removal processes. This set of equations, together with appropriate initial and boundary conditions (in the case of limited-area models), provides the evolution in space and time of emitted trace gases and aerosols mixing ratios.

In general, this set of equations has no analytical solution. It requires numerical methods, parameterizations, and computer resources for an approximated solution through a discretization methodology (e.g., finite differences). The computational limitation implies the use of the so-called "scales separation" of all possible atmospheric motions, which is determined by the chosen space-time discretization. This basically means that the discretization will necessarily separate all the existent atmospheric motion scales in two families: the processes that are explicitly solved (grid scale) and those that are not solved (subgrid scale). However, the nonlinear aspect of the equations involved allows energy exchange between scales and so subgrid processes do generally have a net effect on the grid-scale variables. The accounting for the net effect of subgrid fluxes on the grid scale is achieved by so-called parameterizations, which are undoubtedly simple compared to the highly complex real physical processes they mean to represent. They are usually based on limited observational data sets and on the presently still incomplete level of understanding of interscales exchanges. Thus, physical parameterizations are recognized as an important source of uncertainties in numerical modeling of the atmosphere in general.

The numerical solution for the mass conservation equation (equation (1)) can be achieved through the spatial and temporal discretization and decomposition of the tracer mixing ratio and wind speed into their mean values and fluctuation components (the Reynolds decomposition) [*Stull*, 1988]. Following this approach, equation (1) can be rewritten as

$$\frac{\partial \overline{s_\eta}}{\partial t} + \overline{\vec{v}}.\nabla(\overline{s_\eta}) = -\frac{1}{\rho_0}\nabla.(\rho_0 \overline{s'_\eta \vec{v}'}) + \overline{Q_\eta}. \tag{2}$$

The second term on the left side of equation (2) refers to the advection in the grid scale, and $\overline{Q_\eta}$ is the mean net production in the grid cell by all processes not described as transport. The first term on the right side should include all the subgrid or nonresolved transport mechanisms. Moreover, current computational power does not allow equation (2) to be solved at once, considering all terms simultaneously. The Splitting Operator is a popular technique to do this: instead of solving the full equation at once, it solves each process independently and then couples the various changes resulting from the separate partial solutions [*Yanenko*, 1971; *Seinfeld and Pandis*, 1998; *Lanser and Verwer*, 1998]. It is worth highlighting that in this framework, the solution of equation (2) represents the mean tracer mixing ratio $\overline{s_\eta}$ within the grid volume of finite spatial dimensions (Δx, Δy, Δz). Then, model results must be compared with observational data, taking into account the scale and representativeness of the latter.

Several atmospheric pollutants transport models on regional and global scales have been proposed in the literature. *Chatfield et al.* [1996] used the Global-Regional Atmospheric Chemistry Event Simulator to introduce a conceptual model of fire emissions and chemical production of the African/Oceanic plumes. *Grell et al.* [2000] described a multiscale complex chemistry model coupled to the Penn State/National Center for Atmospheric Research nonhydrostatic mesoscale model (MM5). The Georgia Tech/Goddard Global Ozone Chemistry Aerosol Radiation and Transport (GOCART) model is an example of a global transport model. *Chin et al.* [2000] employed GOCART to simulate the atmospheric global sulfur cycle. Model of Ozone and Related Tracers is an "off-line" global chemical transport model appropriate for simulating the three-dimensional (3-D) distribution of chemical species in the atmosphere

[*Brasseur et al.*, 1998; *Horowitz et al.*, 2003]. More recently, fully coupled "online" regional transport models based on atmospheric models are becoming more common, such as the Coupled Chemistry-Aerosol-Tracer Transport model coupled to Brazilian Regional Atmospheric Modeling System (CCATT-BRAMS) [*Freitas et al.*, 2009; *Longo et al.*, 2007] and the Weather Research and Forecasting Model [*Grell et al.*, 2005; *Fast et al.*, 2006], to name but a few.

CCATT-BRAMS, developed in the context of the LBA program, has been designed to provide a suitable tool to study the atmospheric transport of biomass-burning emissions and their impacts on weather and air quality. It is an Eulerian transport model fully coupled to the BRAMS regional model. The tracer transport simulation is made simultaneously, or "online", with the atmospheric state evolution using exactly the same time step, as well as same dynamics and physical parameterizations. The general mass continuity equation for tracers (in a form of tendency equation and in the context of the Splitting Operator) solved in the CCATT-BRAMS model is:

$$\frac{\partial \bar{s}}{\partial t} = \underbrace{\left(\frac{\partial \bar{s}}{\partial t}\right)_{adv}}_{\mathrm{I}} + \underbrace{\left(\frac{\partial \bar{s}}{\partial t}\right)_{\substack{PBL \\ diff}}}_{\mathrm{II}} + \underbrace{\left(\frac{\partial \bar{s}}{\partial t}\right)_{\substack{deep \\ convn}}}_{\mathrm{III}} + \underbrace{\left(\frac{\partial \bar{s}}{\partial t}\right)_{\substack{shal \\ conv}}}_{\mathrm{IV}} + \underbrace{\left(\frac{\partial \bar{s}}{\partial t}\right)_{\substack{chem \\ reac}}}_{\mathrm{V}} + \underbrace{W}_{\mathrm{VI}} + \underbrace{R}_{\mathrm{VII}} + \underbrace{Q_{pr}}_{\mathrm{VIII}}, \quad (3)$$

where $\bar{s}$ is the grid box mean tracer mixing ratio, term (I) represents the 3-D resolved transport term (advection by the mean wind), term (II) is the subgrid-scale diffusion in the PBL, terms (III) and (IV) are the subgrid transport by deep and shallow convection, respectively. Term (V) is the net production or loss associated to chemical reactions. Term (VI) is the wet removal, term (VII) refers to the dry deposition applied to gases and aerosols particles, and finally, term (VIII) is the source term that includes the plume rise mechanism associated with vegetations fires. Figure 2 illustrates the main subgrid-scale processes involved in biomass-burning smoke trace gases and aerosols transport simulated by the CCATT-BRAMS system. A detailed description of the parameterizations for each one of these processes can be found in the work of *Freitas et al.* [2005, 2007, 2009] and *Longo et al.* [2007].

3.2. Main Processes Related To Smoke Atmospheric Transport

Vegetation fires emit trace gases and aerosol particles to the atmosphere with temperatures much higher than the ambient air and with positive buoyancy, which favors vertical transport. Due to the radiative cooling and the efficient heat transport by convection, there is a rapid decay of temperature above the fire area. Also, the interaction between smoke and the environment produces eddies that entrain colder environmental air into the smoke plume, which dilutes the plume and reduces buoyancy. The dominant characteristic is a strong upward flow with an only moderate temperature

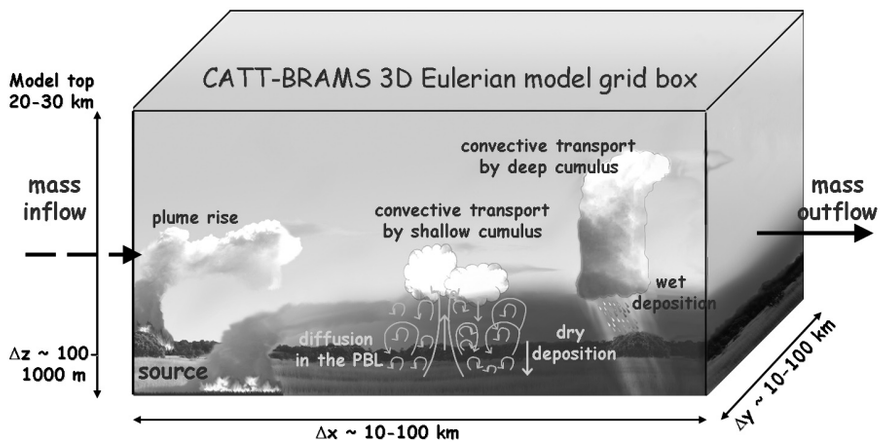

Figure 2. Several subgrid processes involved in gases/aerosols transport and simulated by Coupled Chemistry-Aerosol-Tracer Transport model coupled to Brazilian Regional Atmospheric Modeling System (CCATT-BRAMS) system. Extracted from the work of *Freitas et al.* [2007].

excess above ambient [*Riggan et al.*, 2004]. The final plume height is controlled by the thermodynamic stability of the atmospheric environment and the surface heat flux released from the fire. Moreover, if water vapor reaches condensation, the additional buoyancy gained from the latent heat release plays an important role in determining the effective injection height of the plume [*Freitas et al.*, 2007]. However, the occurrence of strong horizontal winds might enhance the lateral entrainment and even prevent the plume reaching the condensation level, particularly for small fires, impacting on the injection height. Low-density biomass fires, such as burning of cerrado and pastures, typically release smoke into the PBL. On the other hand, forest fires, with high-density vegetation and heat release rate of about 10 GW that typically last for a few hours can inject smoke directly into the low and medium troposphere (3 to 10 km high) and even into the stratosphere developing pyrocumulus [*Fromm et al.*, 2000; *Fromm and Servranckx*, 2003; *Jost et al.*, 2004; *Rosenfeld et al.*, 2006].

Including the plume rise from vegetation fires driven by their own initial buoyancy into regional and global models is a difficult task. In the absence of this mechanism, the pyrogenic emissions often are released at the surface level in the model, or vertically distributed in an arbitrary way [*Turquety et al.*, 2007], or using some empirical relationship between the injection height and fire intensity [*Lavoué et al.*, 2000; *Wang et al.*, 2006]. *Freitas et al.* [2006, 2007] introduced this subgrid process by embedding a 1-D cloud-resolving model with appropriate lower boundary conditions in each column of the 3-D atmospheric model. This 1-D plume model is driven by remote sensing fire location and size, a look-up-table of typical range of heat fluxes, and the updated atmospheric conditions provided by the 3-D host model. This allows the plume rise to be simulated explicitly within each model column with fires, which provides the effective injection height of material emitted during the flaming phase.

On the other hand, the smoke fraction released into the PBL is mixed and vertically transported by turbulence, producing a homogenous mixing layer 1 to 3 km deep during the day. However, dense smoke haze layers can produce a net cooling of the air near the surface and a weakening of the mixing layer turbulence due to solar radiation attenuation, which inhibits the smoke mixing [*Longo et al.*, 2006]. AOD values of 1–3 (500 nm channel) correspond to a negative radiative forcing range of 120–250 Wm^{-2} [*Procópio et al.*, 2004; *Schafer et al.*, 2002b; *Artaxo et al.*, this volume, and references therein]. In fact, AOD observations of the Aerosol Robotic Network sites in Amazonia, with high smoke influence, frequently yield AOD values of up to 3 at 500 nm channel [*Hoelzemann et al.*, 2009].

Shallow and nonprecipitating convective systems over the Amazon basin grow normally on the top of the PBL and, typically, transport gases and particles to the low troposphere enhancing their atmospheric dispersion. The deep convective and precipitating systems, however, act differently, depending on the hygroscopicity properties of the atmospheric constituents. For example, CO_2 and CO, which have low hygroscopicity, are efficiently transported by the ascending stream to the cloud top and detrained into the medium and high troposphere, while carbonaceous aerosol particles are more efficiently absorbed into cloud droplets and scavenged with precipitation. Convective systems also induce the development of descending streams, which bring air parcels from the midtroposphere to dilute and cool the PBL. Several authors [e.g., *Chatfield and Crutzen*, 1984; *Dickerson et al.*, 1987; *Pickering et al.*, 1988; *Thompson et al.*, 1996; *Chatfield et al.*, 1996; *Longo et al.*, 1999; *Andreae et al.*, 2001; *Freitas et al.*, 2000, 2005] have been studying the transport of trace gases and aerosols from biomass burning, with special attention to the atmospheric transport by circulations associated with deep and moist convection. They showed the relevance of these mechanisms on the distribution of pollutants in the medium and high troposphere. The cloud venting is taken into account in regional- or global-scale transport models through cumulus parameterizations normally using the mass flux approach.

The effectiveness of plume rise is comparable with cloud venting by deep moist convection as a mechanism for transporting smoke from the PBL to the upper troposphere, and both are much more effective than shallow convection. A detailed discussion about the relative role of these three smoke vertical transport mechanisms is given by *Freitas et al.* [2007], who compared model results with CO data retrieved by the "Measurements of Pollution in the Troposphere" (MOPITT) instrument, on board the EOS/Terra satellite [*Emmons et al.*, 2004]. Basically, the total absence of any subgrid-scale convective transport in the model results in a heavily polluted PBL and a very clean free troposphere. When only shallow convection is considered, it gives a minor gain in model performance. Even though deep convection allows a better representation of the transport to the upper troposphere, it alone is not enough to describe proper venting from lower to middle levels. The plume rise mechanism alone provides much better results for CO in the PBL and the lower and middle troposphere, but does not allow the upper troposphere to be correctly populated by CO. CO transport models that include all the main vertical transport mechanisms, shallow and deep moist convection, and the pyroconvection induced by vegetation fires, show the best agreement with the MOPITT CO retrieval.

CCATT-BRAMS model simulations of biomass-burning emissions were also evaluated with airborne measurements

of CO within the 5-km column covered by the aircraft [*Freitas et al.*, 2009; *Longo et al.*, 2007] during the LBA field campaigns Smoke, Aerosols, Clouds, Rainfall, and Climate (SMOCC) and Radiation, Cloud, and Climate Interactions in the Amazon (RACCI) that took place in the Amazon basin between mid-September and early November 2002 [*Fuzzi et al.*, 2007]. These model results show that the inclusion of the transport terms described above and represented in equation (3) are sufficient to capture the general pattern of smoke transport either regarding vertical profiling in the PBL and lower troposphere and regional distribution. Although, the model resolution of 35 km did not allow the point-by-point reproduction of the subgrid phenomena effects in the profiling, it did succeed in representing the mean pattern of each airborne profile, with the model results falling within the standard deviation of observations in most of the cases. See the work of *Freitas et al.* [2009] and *Longo et al.* [2007] for details.

During the SMOCC/RACCI campaign, high values of CO and $PM_{2.5}$ were observed near surface level in an Amazonian site under strong influence of fire emissions, Fazenda Nossa Senhora Aparecida (10°45′44″S, 62°21′27″W) near the town Ouro Preto do Oeste in the State of Rondônia. Maximum values of CO and $PM_{2.5}$ observed there were as high as 4000 ppb and 210 μg m^{-3}, respectively. The time series of CO and $PM_{2.5}$ were characterized by strong variability, associated either with the transport of aged smoke and fresh emissions from local fires in the vicinity of the measurement site. *Longo et al.* [2007] have demonstrated that to be able to simulate the observed strong time variability of CO or $PM_{2.5}$ near surface level, it is critical to use daily remote sensing fire counts to correctly ascertain emissions in space and time. The use of climatological or monthly variating emissions results in simulation errors of smoke tracer concentrations concerning both time variability and magnitude.

Horizontally, the atmospheric transport is dominated by advection, which drives the smoke toward the atmospheric flow either in the PBL or free troposphere. To illustrate the long-range transport of biomass-burning emissions, in Plate 2, we show a regional smoke plume covering a considerable part of the SA continent revealed by AOD (channel 550 nm) (a) simulated by CCATT-BRAMS model on 27 August 2002 and (b) retrieved by MODIS-Terra. Smoke emitted from vegetation fires in the Amazon Basin and central Brazil was transported southward following the atmospheric flow in the PBL (see the streamlines at 2 km height in Plate 2a). The approach of a cold front system (not shown) sloped up the low-level polluted air (to typically around 6–10 km high), which was then transported toward the Atlantic Ocean driven by a midlatitude wave train. Model dynamic was able to fairly reproduce the general shape and intensity of this continental smoke plume.

3.3. The General Pattern of Atmospheric Transport of Biomass-Burning Emissions Over South America

The burning season of the SA continent occurs during austral winter. The westward displacement of the South Atlantic Subtropical High (SASH) pressure system and the northward motion of the Intertropical Convergence Zone (ITCZ) establish a high pressure area with little precipitation and light winds in the lower troposphere over the central region of the continent [*Satyamurty et al.*, 1998], synchronized with a shift of the convection in the Amazon basin to the northwestern part of SA. This climatology propitiates the spreading of fires all over SA, and a dense regional plume of smoke covers an area of about 4–5 millions of square kilometers that persists for about 3 months.

The smoke transport mean pattern indeed may be explained in terms of the trade winds, the SASH, and the barrier effect of the Andes Mountains. The position of the SASH determines the inflow of clean maritime air into the biomass-burning area, playing an important role in defining the shape of the regional smoke plume as it is the primary mechanism responsible for the dilution of polluted air. In the northeast region, in spite of the typical huge number of fires, the smoke loading is relatively low due to the continuous venting of clean oceanic air carried by the trade winds, besides the typical low vegetation fuel load. The Andes Mountains on the west side of SA, together with the SASH, impose a long-range transport of smoke from its source areas to the south and southeast of SA, thus disturbing larger areas downwind in the subtropics. Most of the smoke in the lower troposphere is exported to the Atlantic Ocean throughout the southeastern part of the continent driven by the South American Low Level Jet (SALLJ) on the east side of the Andes. The SALLJ is a wind maximum immersed in a poleward warm and moist flow in the low troposphere [see *Nobre et al*., this volume; *Marengo et al*., this volume; *Vera et al.*, 2006]. The episodic interruptions of the SALLJ by cold fronts arriving on subtropical SA are responsible for disturbances in atmospheric stability and in the wind fields defining the latitude of the southeastward smoke flow. These events also periodically cause a phenomenon called friagem [*Marengo et al.*, 1997a, 1997b] that generates frost in southern and southeastern Brazil as well as changes in the wind speed and direction and surface temperature and humidity deep into the north of Amazonia. The episodes of friagems allow the smoke to invade pristine areas of the Amazon basin, with implications for the atmospheric chemistry. The transport of the smoke to the northwestern part of Amazonia toward the convective zone enhances the transport of smoke products to the upper troposphere. In fact, a well-defined regional layer of smoke tracers at the upper levels (~500 hPa) over SA has been

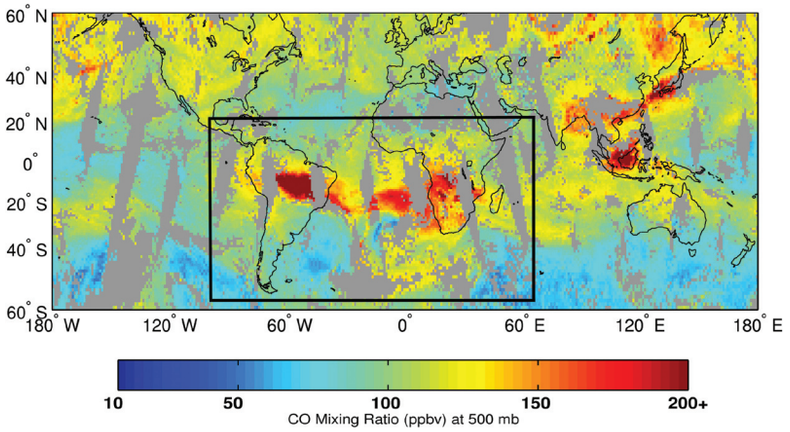

Plate 3. Atmospheric Infrared Sounder 500 hPa CO retrievals (ppbv, color scale) for 22 September 2002 (adapted from *McMillan et al.* [2005]).

observed by airborne measurements as well as by remote sensing [*Andreae et al.*, 2001; *McMillan et al.*, 2005]. A typical pattern for this upper level smoke layer distribution is shown in Plate 3. Modeling studies indicate the deep moist convection and pyroconvection as the key mechanisms acting on this transport [*Freitas et al.*, 2000, 2007; *Andreae et al.*, 2001; *Gevaerd et al.*, 2006]. During the LBA-Cooperative LBA Airborne Regional Experiment (CLAIRE) 1998 field campaign [*Andreae et al.*, 2001], airborne measurements over Suriname sampled a strong polluted layer with

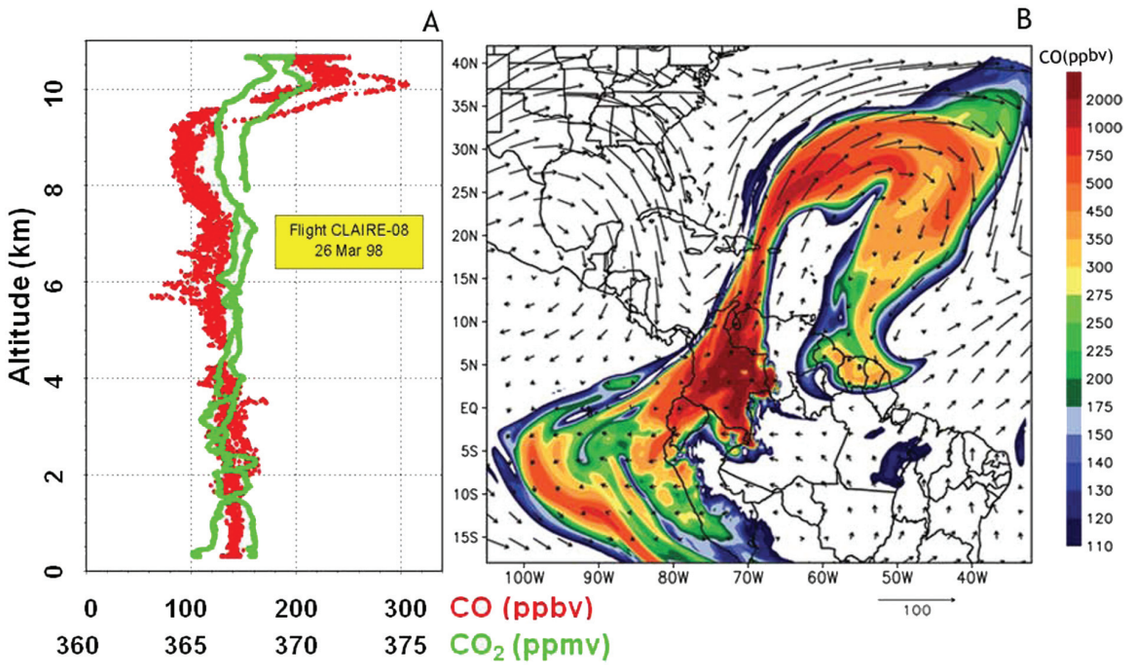

Plate 4. (a) Airborne measurements of (red) CO and (green) CO_2 over Suriname obtained during CLAIRE-08 field campaign [*Andreae et al.*, 2001], and (b) model simulation of biomass-burning CO (ppbv, color scale) around 11 km height on 26 March 1998 from Roraima fires [*Gevaerd et al.*, 2006].

chemical composition characteristic of aged biomass-burning smoke over a clean air column at high altitudes above 9 km on 26 March 1998 (Plate 4a). Back-trajectory analysis indicated that this layer was associated with the emissions from severe wild fires in cerrado and forest areas in Roraima State in the north of Amazonia [*Freitas et al.*, 2000; *Andreae et al.*, 2001]. The fire emissions were advected southwestward in the low troposphere until they got to a deep convection area. The smoke was then entrained into these deep clouds, which transported its low hygroscopic fraction to the upper troposphere (Plate 4b).

In general, the wet deposition resulting from the smoke/cloud interaction processes tends to be associated with local precipitation over Amazonia, but mainly with low level jets or South Atlantic anticyclones, connecting Amazonia and the southern part of South America via biogeochemical cycling of nutrients (Plate 5a). On the other side, the dry deposition of smoke aerosol particles coincides mostly with the biomass-burning emissions area (Plate 5b).

Biomass-burning emissions include ozone precursors that together with natural VOC and plenty of UV radiation in Amazonia efficiently form tropospheric ozone (see section 5.1). The O_3 is produced downwind in the vicinity of fire regions, which typically defines two main corridors of O_3 deposition, following the edge of the Andes Mountains southward and northward (Plate 6). This pattern is associated with events of O_3 and its precursors transport to the north by the cold front approach and to the south by the anticyclone circulation and SALLJ. Over São Paulo state, a corridor is also formed starting from São Paulo metropolitan area, involving mainly reactions of NO_x and VOCs from urban (mainly vehicles source emissions) and rural areas (such as sugar cane burning). These transport and deposition patterns might induce degradation of forest and agricultural areas (such as sugar cane within São Paulo State and soya bean within Mato Grosso State).

4. REGIONAL AND REMOTE IMPACTS OF BIOMASS-BURNING PRODUCTS

In its unperturbed state, the Amazonian atmosphere is characterized by very low concentrations of aerosols and oxidants (Figure 3) [*Andreae et al.*, 2002; *Artaxo et al.*, 2002; *Andreae*, 2008]. The emission of smoke from biomass burning therefore causes dramatic changes in the radiative, cloud physical and chemical properties of the atmosphere over Amazonia, which affect regional climate, ecology, water cycle, and human activities. These changes are summarized in Figure 4, which shows the processes in the atmosphere over the perturbed and smoke-polluted Amazonia. Given the magnitude of burning activity in Amazonia, these perturbations can affect the climate system even on a global scale.

4.1. Impacts on Atmospheric Chemistry

Vast amounts of biogenic VOC are continually emitted from the rainforest into the atmosphere [see *Kesselmeier et al.*, this volume, and references therein]. These compounds are constantly being removed from the atmosphere by oxidation into water-soluble compounds (e.g., polar organics or CO_2) and subsequent surface dry deposition or uptake by cloud drops, snow or ice, followed by precipitation. The most important initial step in the chemical removal mechanisms is the reaction with the hydroxyl radical OH, the atmospheric "detergent" [*Crutzen*, 1995]. The primary hydroxyl radical source is the photodissociation of ozone and subsequent reaction of oxygen atoms with water. OH concentrations are highest in the tropics because of its regime with high levels of UV radiation and water vapor. Most of the oxidation of methane, CO, and other trace gases occurs in the "Great Tropical Reactor," the region of high hydroxyl radical concentrations in the tropical troposphere (Figure 3).

The tropical region, and particularly Amazonia, thus plays a key role not only in regulating physical climate, but also in maintaining the chemical composition of the atmosphere. The reaction with OH radicals is also the dominant sink for methane; therefore, changing OH concentrations also affect the lifetime and thus the atmospheric concentration of this important greenhouse gas.

The relative amounts of hydrocarbons and NO_x play crucial roles in the photochemical oxidation of hydrocarbons. At very low levels of NO_x, a characteristic of the unperturbed Amazon, hydrocarbon oxidation removes ozone and consumes hydroxyl radicals, while at higher NO_x levels, more ozone and reactive radicals are produced [*Butler et al.*, 2008]. Fires emit a huge variety of trace gases (summarized in section 2), comprising the main ingredients of smog chemistry, VOC (including OVOC) and NO_x. The addition of pyrogenic NO_x thus transforms the Amazonian atmosphere from an oxidant-consuming into an oxidant-producing environment and set up the same processes that are active in urban smog. This includes the development of high ozone concentrations, irritant gases such as peroxyacyl (PANs) and acidic components, such as nitric acid and a variety of organic acids [*Browell et al.*, 1990; *Jacob and Wofsy*, 1990; *Kirchhoff et al.*, 1990; *Richardson et al.*, 1991; *Mauzerall et al.*, 1998; *Thompson et al.*, 2001]. In addition to the effects of pyrogenic trace gases, the interaction of smoke aerosols with solar radiation also changes the photolysis rates of key components of the photochemical reaction chains [*Albuquerque et al.*, 2005] and thereby affects atmospheric chemical processes.

Oxidant chemistry, including O_3 formation, begins within the fire plumes from biomass burning [*Andreae et al.*, 1988; *Mauzerall et al.*, 1998] and continues in the regional atmo-

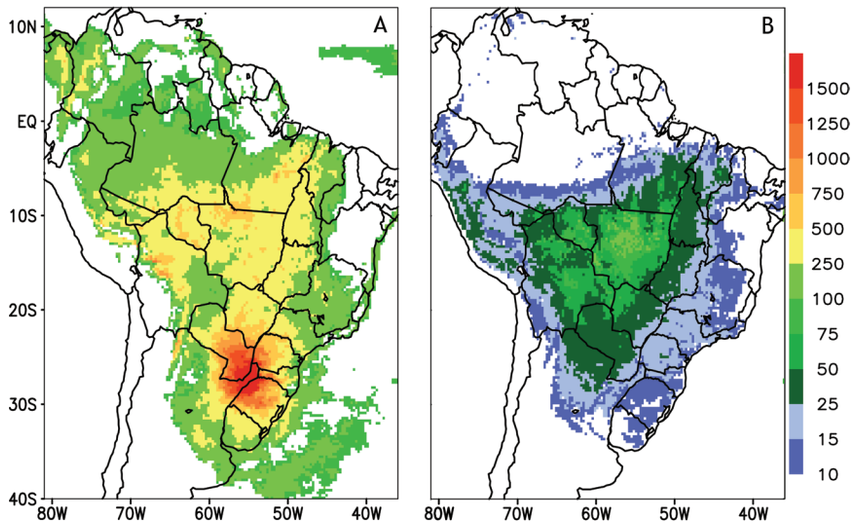

Plate 5. Accumulated (a) wet and (b) dry deposition of smoke aerosol as simulated by CCATT-BRAMS model. The color scale refers to the total amount of aerosol deposited throughout August and September 2002 in mg m^{-2}.

sphere [*Kirchhoff et al.*, 1989, 1990; *Richardson et al.*, 1991]. Ultimately, air masses containing elevated ozone concentrations are exported from the SA continent over the Pacific and Atlantic oceans, and even to other continents, especially Southern Africa. This leads to seasonally very high ozone concentrations, especially over the central South Atlantic [*Fishman et al.*, 1996; *Thompson et al.*, 1996, 2001].

As a result of the smog chemistry caused by pyrogenic emissions, the Amazonian forest is subjected to substantial deposition of nutrients, but also plant-toxic compounds, especially O_3 [*Gut et al.*, 2002; *Kirkman et al.*, 2002; *Rummel et al.*, 2002, 2007]. The deposition of OVOC species, such as organic acids and aldehydes, is also elevated during the fire season [*Kesselmeier et al.*, 2002; *Kuhn et al.*, 2002]. Ozone concentrations over forests during the burning season are sufficiently high that they must be expected to reduce plant primary productivity. On the other hand, nitrogen deposition may have some fertilizing effect to the remaining rainforest, albeit at the expense of the forest that has been burned elsewhere. In general, extremely bad air quality conditions persist during 90% of the burning season period, causing health problems in the exposed communities [*Ignotti et al.*, 2007, 2009].

4.2. Impacts on Atmospheric Radiation, Photosynthesis, and Radiative Forcing

The dramatically elevated concentrations of aerosol particles in the Amazonian atmosphere during the fire season [*Talbot et al.*, 1988; *Echalar et al.*, 1998; *Artaxo et al.*, 2002] results in a sharp increase in scattering and absorption of incoming sunlight. This is evident in an increase of aerosol optical thickness (a measure of the extinction of sunlight by aerosols) from values around 0.05–0.08 in the wet season to

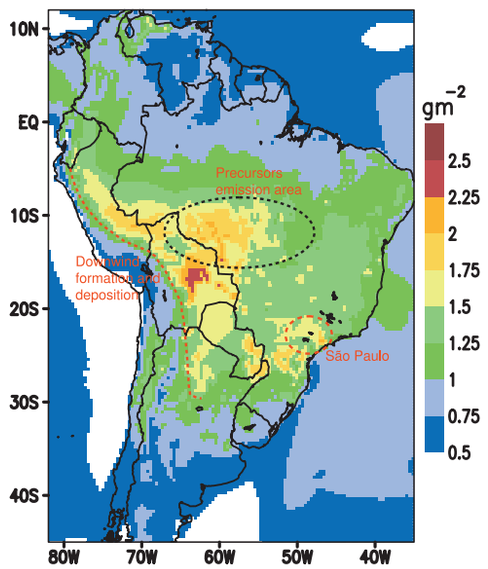

Plate 6. Accumulated deposition of O_3 as simulated by CCATT-BRAMS model. The color scale refers to the total amount of ozone deposited throughout August and September 2002 in 10^{-3} kg m^{-2}.

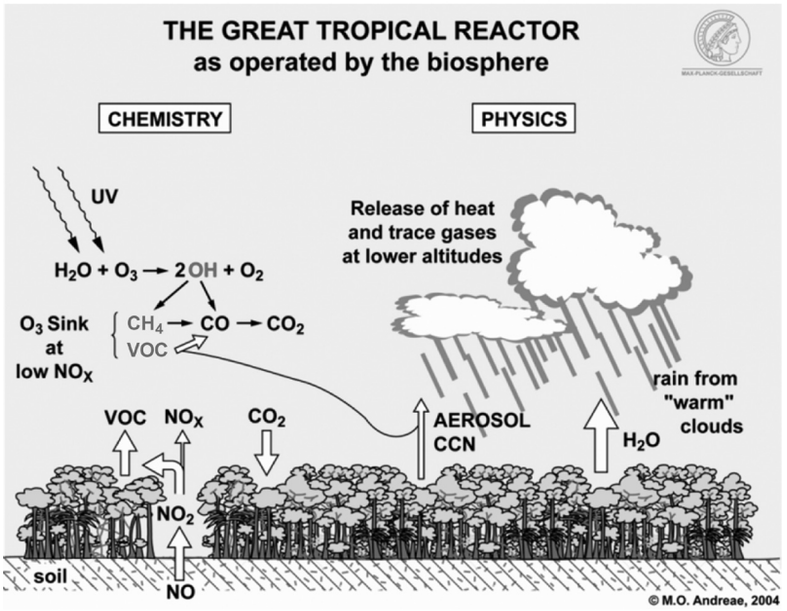

Figure 3. The great tropical reactor as operated by the biosphere. Copyright M. O. Andreae, 2004. Reprinted with permission.

0.9 or more in the fire season [*Andreae*, 2008; *Schafer et al.*, 2008]. The perturbation of solar radiation flux by pyrogenic aerosols affects vegetation by changing the light climate to which plants are exposed and thereby the carbon budget of the Amazon Basin. It also affects the energy budgets of the surface and troposphere, and thus causes direct radiative forcing of climate and modification of cloud processes and precipitation. Finally, aerosols also influence atmospheric photochemistry by changing the radiative flux and thus the photolysis rates of important chemical species such as O_3

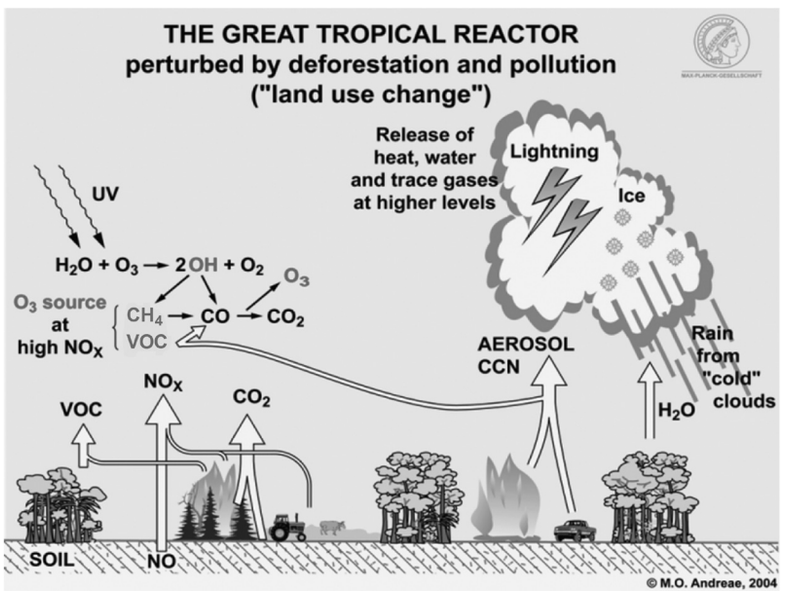

Figure 4. The great tropical reactor perturbed by deforestation and pollution. Copyright M. O. Andreae, 2004. Reprinted with permission.

and NO_2 [*Dickerson et al.*, 1997; *Castro et al.*, 2001; *Albuquerque et al.*, 2005].

By scattering light back to space and by absorbing light, aerosols reduce the amount of direct solar radiation available for plant photosynthesis. On the other hand, some of the scattered light is scattered in the forward direction and arrives on the canopy in the form of diffuse radiation. Overall, the canopy thus receives less light, but at a higher ratio of diffuse to direct radiation [*Schafer et al.*, 2002a, 2002b, 2008]. This results in a complex response of photosynthesis to increasing aerosol levels, as less light becomes available to the leaves at the top of the canopy, but more light reaches the "shade leaves" that only receive diffuse radiation. As a result, net primary production initially increases with increasing aerosol load, but then decreases again at even higher aerosol burdens [*Yamasoe et al.*, 2006; *Oliveira et al.*, 2007].

The presence of an aerosol layer reduces the amount of solar energy arriving at the surface and thereby produces a negative (cooling) radiative forcing at the surface. Values of −20 to −70 W m^{-2} have been reported for this forcing in Amazonia [*Ross et al.*, 1998; *Procópio et al.*, 2004]. On the other hand, the absorption of light by the light-absorbing carbon (LAC) component of the smoke aerosol [*Andreae and Gelencsér*, 2006] leads to a warming of the tropospheric layers in which the smoke resides. This results in a stabilization of the atmosphere and consequently a reduction of cloudiness [*Feingold et al.*, 2005; *Longo et al.*, 2006; *Zhang et al.*, 2008]. Because of the high reflectivity of the smoke aerosols, they reflect more light back to space than the unpolluted Amazonian atmosphere, provoking a net cooling forcing to the radiation budget measured at the top of the atmosphere. During the dry season, this forcing is of the order of −5 to −12 W m^{-2} [*Procópio et al.*, 2004]. Thus, the net effect of smoke aerosols is a cooling forcing that is quite pronounced at the local and regional scale, and even significant for global climate [*Robock*, 1991].

4.3. Impacts on Clouds and Precipitation

The effect of pyrogenic aerosols on the surface and atmospheric radiation budget has already been mentioned in the previous section. The resulting suppression of cloudiness is further enhanced by the "cloud burning" effect of LAC particles inside cloud air and cloud droplets, which leads to a warming inside the cloud, in general, and the droplets, in particular. This causes clouds to evaporate even when they have formed in spite of the reduction of surface heating, an effect that has been observed by remote sensing over Amazonia [*Koren et al.*, 2004]. Overall, the radiative effect of smoke aerosols on clouds leads to reduced cloudiness (particularly for small clouds), a delayed transition from dry to wet season, and changes in the basin-scale patterns of wind divergence and convergence [*Silva Dias et al.*, 2002; *Zhang et al.*, 2008].

As aerosols also act as cloud condensation nuclei (CCN), they are able to change the microphysical behavior of clouds and, consequently, also their dynamics and precipitation efficiency [*Rosenfeld et al.*, 2008; *Martins et al*, 2009]. Over Amazonia, the large differences in CCN concentration between wet and dry season lead to pronounced changes in cloud microphysical properties, especially the droplet effective radius [*Roberts et al.*, 2003; *Kaufman and Nakajima*, 1993; *Feingold et al.*, 2001]. This increases the reflectivity of the clouds and has a cooling effect on climate. It also reduces the rate at which cloud droplets can grow to raindrops in those parts of the cloud that are below the freezing level. The change in microphysical properties also induces a reduction or complete suppression of rainfall from relatively shallow ("warm") clouds [*Andreae et al.*, 2004; *Rosenfeld et al.*, 2008; *Silva Dias et al.*, 2002].

The suppression of early rain from the "warm" part of the clouds allows more of the water vapor to ascend to the freezing level and above, where more water can condense because of the lower temperature of condensation. Furthermore, the latent heat of freezing is released in addition to the latent heat of condensation. Both of these effects result in an invigoration of cloud dynamics and an intensification of precipitation [*Rosenfeld et al.*, 2008; *Martins et al.*, 2009]. At even higher aerosol concentrations, the formation of precipitation is suppressed even in cold clouds, and the cooling radiative effect of the aerosol reduces the energy available for convection. Consequently, the invigoration of convection and precipitation by aerosols has a maximum at intermediate aerosol concentrations around 1000–3000 cm^{-3}. Observational support for this conceptual model has been found over Amazonia by remote sensing studies [*Lin et al.*, 2006; *Koren et al.*, 2008].

The increase in the role of the mixed-phase region in clouds (i.e., the region where water and ice phase coexist) by aerosol microphysical effects also has consequences on the type and amount of lightning activity. Studies in Amazonia have shown an increased lightning activity under the presence of biomass smoke [*Williams et al.*, 2002; *Andreae et al.*, 2004]. Due to their chemical composition, smoke aerosols also enhance the frequency of positive cloud-to-ground lightning strokes [*Lyons et al.*, 1998; *Fernandes et al.*, 2006].

4.4. Global Effects

The implications of biomass burning in Amazonia for global climate and atmospheric composition remain to be fully

explored. Obviously, during years of very extensive burning due to climatic variability (El Niño) or extreme deforestation rates, the enhanced emissions of greenhouse gases are seen as interannual variations in the growth rate of CO_2, CH_4, etc. [*Langenfelds et al.*, 2002]. Teleconnections resulting from perturbation of convection dynamics are difficult to explore at this time because of the inadequate parameterization of aerosol effects on clouds and precipitation in global models, but initial studies have shown significant effects [*Nober et al.*, 2003]. Due to the fact that burning predominantly takes place in the trade wind region, a substantial part of the emissions are transported toward the ITCZ, where they can become subjected to deep convection and transported into the upper troposphere and the tropical transition layer [*Freitas et al.*, 2000; *Andreae et al.*, 2001]. Enhancement of convection by the mechanisms discussed above and the suppression of scavenging at very high aerosol levels make the vertical transport of smoke particularly effective. While a large fraction of aerosols is removed by scavenging during these convection events, even a modest fraction of surviving smoke aerosols can make an important contribution to the aerosol budget of the very clean upper troposphere. The same applies to reactive pyrogenic trace gases, e.g., acetone and formaldehyde, which can play important roles in the chemistry of the upper troposphere.

Acknowledgment. The authors would like to thank Judith Hoelzemann for the final revision of the manuscript.

REFERENCES

Albuquerque, L. M. M., K. M. Longo, S. R. Freitas, T. Tarasova, A. Plana Fattori, C. Nobre, and L. V. Gatti (2005), Sensitivity studies on the photolysis rates calculation in Amazonian atmospheric chemistry—Part I: The impact of the direct radiative effect of biomass burning aerosol particles, *Atmos. Chem. Phys. Disc.*, *5*, 9325–9353.

Andrade, S. M. A., W. N. Neto, and H. S. Miranda (1999), The dynamics of components of the fine fuel after recurrent prescribed fires in Central Brazil savannas, Proceedings of the Bushfire 99 Conference, Alburn, Australia.

Andreae, M. O. (2008), Correlation between cloud condensation nuclei concentration and aerosol optical thickness in remote and polluted regions, *Atmos. Chem. Phys. Disc.*, *8*, 11,293–11, 320.

Andreae, M. O., and A. Gelencsér (2006), Black carbon or brown carbon? The nature of light-absorbing carbonaceous aerosols, *Atmos. Chem. Phys.*, *6*, 3131–3148.

Andreae, M. O., and P. Merlet (2001), Emission of trace gases and aerosols from biomass burning, *Global Biogeochem. Cycles*, *15*(4), 955–966.

Andreae, M. O., et al. (1988), Biomass-burning emissions and associated haze layers over Amazonia, *J. Geophys. Res.*, *93*, 1509–1527.

Andreae, M. O., et al. (2001), Transport of biomass burning smoke to the upper troposphere by deep convection in the equatorial region, *Geophys. Res. Lett.*, *28*, 951–954.

Andreae, M. O., et al. (2002), Biogeochemical cycling of carbon, water, energy, trace gases, and aerosols in Amazonia: The LBA-EUSTACH experiments, *J. Geophys. Res.*, *107*(D20), 8066, doi:10.1029/2001JD000524.

Andreae, M. O., D. Rosenfeld, P. Artaxo, A. A. Costa, G. P. Frank, K. M. Longo, and M. A. F. Silva-Dias (2004), Smoking rain clouds over the Amazon, *Science*, *303*, 1337–1342.

Artaxo, P., E. T. Fernandes, J. V. Martins, M. A. Yamasoe, P. V. Hobbs, W. Maenhaut, K. M. Longo, and A. Castanho (1998), Large-scale aerosol source apportionment in Amazonia, *J. Geophys. Res.*, *103*, 31,837–31,847.

Artaxo, P., J. V. Martins, M. A. Yamasoe, A. S. Procópio, T. M. Pauliquevis, M. O. Andreae, P. Guyon, L. V. Gatti, and A. M. C. Leal (2002), Physical and chemical properties of aerosols in the wet and dry seasons in Rondônia, Amazonia, *J. Geophys. Res.*, *107*(D20), 8081, doi:10.1029/2001JD000666.

Artaxo, P., et al. (2009), Aerosol particles in Amazonia: Their composition, role in the radiation balance, cloud formation, and nutrient cycles, *Geophys. Monogr. Ser.*, doi:10.1029/2008GM000778, this volume.

Barbosa, R. I., and P. M. Fearnside (1996), Pasture burning in Amazonia: Dynamics of residual biomass and the storage and release of aboveground carbon, *J. Geophys. Res.*, *101*(D20), 25,847–25,857.

Bergamaschi, P., R. Hein, C. A. M. Brenninkmeijer, and P. J. Crutzen (2000), Inverse modeling of the global CO cycle 2. Inversion of $^{13}C/^{12}C$ and $^{18}O/^{16}O$ isotope ratios, *J. Geophys. Res.*, *105*(D2), 1929–1945.

Bertschi, I. T., R. J. Yokelson, D. E. Ward, R. E. Babbitt, R. A. Susott, J. G. Goode, and W. M. Hao (2003), Trace gas and particle emissions from fires in large diameter and belowground biomass fuels, *J. Geophys. Res.*, *108*(D13), 8472, doi:10.1029/2002JD002100.

Blake, N. J., D. R. Blake, B. C. Sive, T.-Y. Chen, F. S. Rowland, J. E. Collins, G. W. Sachse, and B. E. Anderson (1996), Biomass burning emissions and vertical distribution of atmospheric methyl halides and other reduced carbon gases in the South Atlantic region, *J. Geophys. Res.*, *101*, 24,151–24,164.

Brasseur, G. P., D. A. Hauglustaine, S. Walters, R. J. Rasch, J.-F. Müller, C. Granier, and X. X. Tie (1998), MOZART, a global chemical transport model for ozone and related chemical tracers 1: Model description, *J. Geophys. Res.*, *103*(D21), 28,265–28,289.

Browell, E. V., G. L. Gregory, R. C. Harriss, and V. W. J. H. Kirchhoff (1990), Ozone and aerosol distributions over the Amazon Basin during the wet season, *J. Geophys. Res.*, *95*(D10), 16,887–16,901.

Butler, T. M., D. Taraborrelli, C. Bruehl, H. Fischer, H. Harder, M. Martinez, J. Williams, M. G. Lawrence, and J. Lelieveld (2008), Improved simulation of isoprene oxidation chemistry with the ECHAM5/MESSy chemistry-climate model: Lessons from the

GABRIEL airborne field campaign, *Atmos. Chem. Phys.*, *8*, 4529–4546.

Câmara, G., A. P. D. Aguiar, M. I. Escada, S. Amaral, T. Carneiro, A. M. Monteiro, R. Araújo, I. Vieira, and B. Becker (2005), Amazonian deforestation models, *Science*, *307*(5712), 1043–1044.

Carvalho, J. A., Jr., N. Higuchi, T. M. Araújo, and J. C. Santos (1998), Combustion completeness in a rainforest clearing experiment in Manaus, Brazil, *J. Geophys. Res.*, *103*(D11), 13,195–13,199.

Carvalho, J. A., Jr., F. S. Costa, C. A. Gurgel Veras, D. V. Sandberg, E. C. Alvarado, R. Gielow, A. M. Serra Jr., and J. C. Santos (2001), Biomass fire consumption and carbon release rates of rainforest-clearing experiments conducted in northern Mato Grosso, Brazil, *J. Geophys. Res.*, *106*(D16), 17,877–17,887.

Castro, T., S. Madronich, S. Rivale, A. Muhlia, and B. Mar (2001), The influence of aerosols on photochemical smog in Mexico City, *Atmos. Environ.*, *35*, 1765–1772.

Chand, D., P. Guyon, P. Artaxo, O. Schmid, G. P. Frank, L. V. Rizzo, O. L. Mayol-Bracero, L. V. Gatti, and M. O. Andreae (2006), Optical and physical properties of aerosols in the boundary layer and free troposphere over the Amazon Basin during the biomass burning season, *Atmos. Chem. Phys.*, *6*, 2911–2925.

Chatfield, R. B., and P. J. Crutzen (1984), Sulfur dioxide in remote oceanic air: Cloud transport of reactive precursors, *J. Geophys. Res.*, *89*(D5), 7111–7132.

Chatfield, R. B., J. A. Vastano, H. B. Singh, and G. Sachse (1996), A general model of how fire emissions and chemistry produce African/oceanic plumes (O_3, CO, PAN, smoke), *J. Geophys. Res.*, *101*(D19), 24,279–24,306.

Chin, M., R. B. Rood, S.-J. Lin, J.-F. Müller, and A. M. Thompson (2000), Atmospheric sulfur cycle simulated in the global model GOCART: Model description and global properties, *J. Geophys. Res.*, *105*, 24,671–24,687.

Christian, T., B. Kleiss, R. J. Yokelson, R. Holzinger, P. J. Crutzen, W. M. Hao, B. H. Saharjo, and D. E. Ward (2003), Comprehensive laboratory measurements of biomass-burning emissions: 1. Emissions from Indonesian, African, and other fuels, *J. Geophys. Res.*, *108*(D23), 4719, doi:10.1029/2003JD003704.

Christian, T. J., R. J. Yokelson, J. A. Carvalho Jr., D. W. T. Griffith, E. C. Alvarado, J. C. Santos, T. G. S. Neto, C. A. G. Veras, and W. M. Hao (2007), The tropical forest and fire emissions experiment: Trace gases emitted by smoldering logs and dung from deforestation and pasture fires in Brazil, *J. Geophys. Res.*, *112*, D18308, doi:10.1029/2006JD008147.

Coutinho, L. M. (1990), Fire in the ecology of the Brazilian cerrado, in *Fire in the Tropical Biota: Ecosystem Processes and Global Challenges*, edited by J. G. Goldammer, pp. 82–105, Springer, Berlin.

Crutzen, P. J. (1995), Overview of tropospheric chemistry: Developments during the past quarter century and a look ahead, *Faraday Discuss.*, *100*, 1–21.

Crutzen, P. J., and M. O. Andreae (1990), Biomass burning in the tropics: Impact on atmospheric chemistry and biogeochemical cycles, *Science*, *250*, 1669–1678.

Dickerson, R. R., et al. (1987), Thunderstorms: An important mechanism in the transport of air pollutants, *Science*, *235*, 460–465.

Dickerson, R. R., S. Kondragunta, G. Stenchikov, K. L. Civerolo, B. G. Doddridge, and B. N. Holben (1997), The impact of aerosols on solar ultraviolet radiation and photochemical smog, *Science*, *278*, 827–830.

Duncan, B. N., R. V. Martin, A. C. Staudt, R. Yevich, and J. A. Logan (2003), Interannual and seasonal variability of biomass burning emissions constrained by satellite observations, *J. Geophys. Res.*, *108*(D2), 4100, doi:10.1029/2002JD002378.

Echalar, F., P. Artaxo, J. V. Martins, M. A. Yamasoe, F. Gerab, W. Maenhaut, and B. Holben (1998), Long-term monitoring of atmospheric aerosols in the Amazon Basin: Source identification and apportionment, *J. Geophys. Res.*, *103*, 31,849–31,864.

Emmons, L. K., et al. (2004), Validation of Measurements of Pollution in the Troposphere (MOPITT) CO retrievals with aircraft in situ profiles, *J. Geophys. Res.*, *109*, D03309, doi:10.1029/2003JD004101.

Fast, J. D., W. I. Gustafson Jr., R. C. Easter, R. A. Zaveri, J. C. Barnard, E. G. Chapman, G. A. Grell, and S. E. Peckham (2006), Evolution of ozone, particulates, and aerosol direct radiative forcing in the vicinity of Houston using a fully coupled meteorology-chemistry-aerosol model, *J. Geophys. Res.*, *111*, D21305, doi:10.1029/2005JD006721.

Fearnside, P. M. (1990), Fire in the tropical rain forest of the Amazon basin, in *Fire in the Tropical Biota: Ecosystem Processes and Global Challenges*, edited by J. G. Goldammer, pp. 106–116, Springer, Berlin.

Fearnside, P. M., N. Leal Jr., and F. M. Fernandes (1993), Rainforest burning and the global budget: Biomass, combustion efficiency, and charcoal formation in the Brazilian Amazon, *J. Atmos. Chem.*, *98*, 733–743.

Feingold, G., L. A. Remer, J. Ramaprasad, and Y. J. Kaufman (2001), Analysis of smoke impact on clouds in Brazilian biomass burning regions: An extension of Twomey's approach, *J. Geophys. Res.*, *106*, 22,907–22,922.

Feingold, G., H. Jiang, and J. Y. Harrington (2005), On smoke suppression of clouds in Amazonia, *Geophys. Res. Lett.*, *32*, L02804, doi:10.1029/2004GL021369.

Ferek, R. J., J. S. Reid, P. V. Hobbs, D. R. Blake, and C. Liousse (1998), Emission factors of hydrocarbons, halocarbons, trace gases, and particles from biomass burning in Brazil, *J. Geophys. Res.*, *103*(D24), 32,107–32,118.

Fernandes, W. A., I. R. C. A. Pinto, O. Pinto Jr., K. M. Longo, and S. R. Freitas (2006), New findings about the influence of smoke from fires on the cloud-to-ground lightning characteristics in the Amazon region, *Geophys. Res. Lett.*, *33*, L20810, doi:10.1029/2006GL027744.

Fishman, J., V. G. Brackett, E. V. Browell, and W. B. Grant (1996), Tropospheric ozone derived from TOMS/SBUV measurements during TRACE A, *J. Geophys. Res.*, *101*, 24,069–24,082.

Freitas, S. R., M. A. F. S. Dias, P. L. S. Dias, K. M. Longo, P. Artaxo, M. O. Andreae, and H. Fischer (2000), A convective kinematic trajectory technique for low-resolution atmospheric models, *J. Geophys. Res.*, *105*(D19), 24,375–24,386.

Freitas, S. R., K. M. Longo, M. Silva Dias, P. Silva Dias, R. Chatfield, E. Prins, P. Artaxo, G. Grell, and F. Recuero (2005), Monitoring the transport of biomass burning emissions in South

America, *Environ. Fluid Mech.*, *5*(1–2), 135–167, doi:10.1007/s10652-005-0243-7.

Freitas, S. R., K. M. Longo, and M. O. Andreae (2006), Impact of including the plume rise of vegetation fires in numerical simulations of associated atmospheric pollutants, *Geophys. Res. Lett.*, *33*, L17808, doi:10.1029/2006GL026608.

Freitas, S. R., K. M. Longo, R. Chatfield, D. Latham, M. A. F. Silva Dias, M. O. Andreae, E. Prins, J. C. Santos, R. Gielow, and J. A. Carvalho Jr. (2007), Including the sub-grid scale plume rise of vegetation fires in low resolution atmospheric transport models, *Atmos. Chem. Phys.*, *7*, 3385–3398.

Freitas, S. R., et al. (2009), The Coupled Aerosol and Tracer Transport model to the Brazilian developments on the Regional Atmospheric Modeling System. Part 1: Model description and evaluation, *Atmos. Chem. Phys.*, *9*, 2843–2861.

Fromm, M. D., and R. Servranckx (2003), Transport of forest fire smoke above the tropopause by supercell convection, *Geophys. Res. Lett.*, *30*(10), 1542, doi:10.1029/2002GL016820.

Fromm, M., J. Alfred, K. Hoppel, J. Hornstein, R. Bevilacqua, E. Shettle, R. Servranckx, Z. Li, and B. Stocks (2000), Observations of boreal forest fire smoke in the stratosphere by POAM III, SAGE II, and lidar in 1998, *Geophys. Res. Lett.*, *27*, 1407–1410.

Fuzzi, S., et al. (2007), Overview of the inorganic and organic composition of size-segregated aerosol in Rondônia, Brazil, from the biomass burning period to the onset of the wet season, *J. Geophys. Res.*, *112*, D01201, doi:10.1029/2005JD006741.

Gevaerd, R.; S. R. Freitas, and K. M. Longo (2006), Numerical simulation of biomass burning emission and transportation during 1998 Roraima fires [CD-ROM], in *Proceedings of 8th International Conference on Southern Hemisphere Meteorology and Oceanography (ICSHMO), Foz do Iguaçu, Brazil, 24–28 April*, pp. 883–889, INPE, São José dos Campos, ISBN 85-17-00023-4.

Giglio, L., G. R. van der Werf, J. T. Randerson, G. J. Collatz, and P. Kasibhatla (2006), Global estimation of burned area using MODIS active fire observations, *Atmos. Chem. Phys.*, *6*, 957–974.

Greenberg, J. P., P. R. Zimmerman, L. Heidt, and W. Pollock (1984), Hydrocarbon and carbon monoxide emissions from biomass burning in Brazil, *J. Geophys. Res.*, *89*, 1350–1354.

Grell, G., S. Emeis, W. Stockwell, T. Schoenemeyer, R. Forkel, J. Michalakes, R. Knoche, and W. Seidl (2000), Application of a multiscale, coupled MM5/chemistry model to the complex terrain of the VOTALP valley campaign, *Atmos. Environ.*, *34*, 1435–1453.

Grell, G., S. Peckham, R. Schmitz, S. McKeen, G. Frost, W. Skamarock, and B. Eder (2005), Fully coupled "online" chemistry within the WRF model, *Atmos. Environ.*, *39*(37), 6957–6975.

Guild, L. S., J. B. Kaufmann, L. J. Ellingson, D. L. Cummings, E. A. Castro, R. E. Babbitt, and D. E. Ward (1998), Dynamics associated with total above ground biomass, C, nutrient pools, and biomass burning of primary forest and pasture in Rondônia, Brazil during SCAR-B, *J. Geophys. Res.*, *103*, 32,091–32,100.

Gut, A., et al. (2002), Exchange fluxes of NO_2 and O_3 at soil and leaf surfaces in an Amazonian rain forest, *J. Geophys. Res.*, *107*(D20), 8060, doi:10.1029/2001JD000654.

Guyon, P., et al. (2005), Airborne measurements of trace gases and aerosol particle emissions from biomass burning in Amazonia, *Atmos. Chem. Phys.*, *5*, 2989–3002.

Hao, W. M., and M.-H. Liu (1994), Spatial and temporal distribution of tropical biomass burning, *Global Biogeochem. Cycles*, *8*(4), 495–503.

Hobbs, P. V., J. S. Reid, R. A. Kotchenruther, R. J. Ferek, and R. Weiss (1997), Direct radiative forcing by smoke from biomass burning, *Science*, *275*, 1777–1778.

Hobbs, P. V., P. Sinha, R. J. Yokelson, T. J. Christian, D. R. Blake, S. Gao, T. W. Kirchstetter, T. Novakov, and P. Pilewskie (2003), Evolution of gases and particles from a savanna fire in South Africa, *J. Geophys. Res.*, *108*(D13), 8485, doi:10.1029/2002JD002352.

Hoelzemann, J. J. (2007), *Global Wildland Fires Impact on Atmospheric Chemistry*, 200 pp., VDM-Verlag Dr. Müller, Saarbruecken, Germany.

Hoelzemann, J. J., M. G. Schultz, G. P. Brasseur, C. Granier, and M. Simon (2004), Global Wildland Fire Emission Model (GWEM): Evaluating the use of global area burnt satellite data, *J. Geophys. Res.*, *109*, D14S04, doi:10.1029/2003JD003666.

Hoelzemann, J. J., K. M. Longo, R. M. Fonseca, N. M. E. do Rosário, H. Elbern, S. R. Freitas, and C. Pires (2009), Regional representativity of AERONET observation sites during the biomass burning season in South America determined by correlation studies with MODIS Aerosol Optical Depth, *J. Geophys. Res.*, *114*, D13301, doi:10.1029/2008JD010369.

Horowitz, L. W., et al. (2003), A global simulation of tropospheric ozone and related tracers: Description and evaluation of MOZART, version 2, *J. Geophys. Res.*, *108*(D24), 4784, doi:10.1029/2002JD002853.

Ichoku, C., and Y. J. Kaufman (2005), A method to derive smoke emission rates from MODIS fire radiative energy measurements, *IEEE Trans. Geosci. Remote Sens.*, *43*(11), 2636–2649.

Ignotti, E., S. Hacon, A. M. Silva, W. L. Junger, and H. A. Castro (2007), Effects of biomass burning in Amazon: Method to select municipalities using health indicators, *Rev. Bras. Epidemiol.*, *10*, 453–464.

Ignotti, E., I. Valente, S. Hacon, K. M. Longo, S. R. Freitas, and P. Artaxo (2009), Impacts of particulate matter ($PM_{2.5}$) emitted from biomass burning in the Amazon regarding hospital admissions by respiratory diseases: Building up environmental indicators and a new methodological approach (online), *Rev. Saude Publica*, in press.

Instituto Nacional de Pesquisas Espaciais (INPE) (2008), Monitoramento da cobertura florestal da Amazônia por satélites Sistemas PRODES, DETER, DEGRAD e QUEIMADAS 2007–2008, report, Coord. Geral de Obs. da Terra, Minist. da Ciência e Tecnol., São José dos Campos, Brazil. (Available at http://www.obt.inpe.br/prodes/Relatorio_Prodes2008.pdf).

Jacob, D. J., and S. C. Wofsy (1990), Budgets of reactive nitrogen, hydrocarbons, and ozone over the Amazon forest during the wet season, *J. Geophys. Res.*, *95*, 16,737–16,754.

Jost, H.-J., et al. (2004), In-situ observations of mid-latitude forest fire plumes deep in the stratosphere, *Geophys. Res. Lett.*, *31*, L11101, doi:10.1029/2003GL019253.

Karl, T. G., T. J. Christian, R. J. Yokelson, P. Artaxo, W. M. Hao, and A. Guenther (2007), The tropical forest and fire emissions experiment: Method evaluation of volatile organic compound emissions measured by PTR-MS, FTIR, and GC from tropical biomass burning, *Atmos. Chem. Phys.*, *7*, 5883–5897.

Kauffman, J. B., D. L. Cummings, and D. E. Ward (1994), Relationships of fire, biomass and nutrient dynamics along a vegetation gradient in the Brazilian cerrado, *J. Ecol.*, *82*, 519–531.

Kauffman, J. B., D.L. Cummings, and D.E. Ward (1998), Fire in the Brazilian Amazon 2. Biomass, nutrient pools and losses in cattle pastures, *Oecologia*, *113*, 415–427, doi:10.1007/s004420050394.

Kaufman, Y., and I. Koren (2006), Smoke and pollution aerosol effect on cloud cover, *Science*, *313*, 655–658, doi:10.1126/science.1126232.

Kaufman, Y., C. Ichoku, L. Giglio, S. Korontzi, D. A. Chu, W. M. Hao, R.-R. Li, and C. O. Justice (2003) Fires and smoke observed from the Earth Observing System MODIS instrument: Products, validation, and operational use, *Int. J. Remote Sens.*, *24*, 1765–1781.

Kaufman, Y. J., and T. Nakajima (1993), Effect of Amazon smoke on cloud microphysics and albedo—Analysis from satellite imagery, *J. Appl. Meteorol.*, *32*, 729–744.

Kaufman, Y. J., et al. (1998), Smoke, Clouds, and Radiation-Brazil (SCAR-B) experiment, *J. Geophys. Res.*, *103*(D24), 31,783–31,808.

Kesselmeier, J., et al. (2002), Concentrations and species composition of atmospheric volatile organic compounds (VOCs) as observed during the wet and dry season in Rondônia (Amazonia), *J. Geophys. Res.*, *107*(D20), 8053, doi:10.1029/2000JD000267.

Kesselmeier, J., A. Guenther, T. Hoffmann, M. T. Piedade, and J. Warnke (2009), Natural volatile organic compound emissions from plants and their roles in oxidant balance and particle formation, *Geophys. Monogr. Ser*., doi:10.1029/2008GM000717, this volume.

Kirchhoff, V. W. J. H., A. W. Setzer, and M. C. Pereira (1989), Biomass burning in Amazonia: Seasonal effects on atmospheric O_3 and CO, *Geophys. Res. Lett.*, *16*, 469–472.

Kirchhoff, V. W. J. H., I. M. O. da Silva, and E. V. Browell (1990), Ozone measurements in Amazonia: Dry season versus wet season, *J. Geophys. Res.*, *95*, 16,913–16,926.

Kirkman, G. A., A. Gut, C. Ammann, L. V. Gatti, A. M. Cordova, M. A. L. Moura, M. O. Andreae, and F. X. Meixner (2002), Surface exchange of nitric oxide, nitrogen dioxide, and ozone at a cattle pasture in Rondônia, Brazil, *J. Geophys. Res.*, *107*(D20), 8083, doi:10.1029/2001JD000523.

Kley, D. (1997), Tropospheric chemistry and transport, *Science*, *276*, 1043–1045.

Koren, I., Y. J. Kaufman, L. A. Remer, and J. V. Martins (2004), Measurement of the effect of Amazon smoke on inhibition of cloud formation, *Science*, *303*, 1342–1345.

Koren, I., J. V. Martins, L. A. Remer, and H. Afargan (2008), Smoke invigoration versus inhibition of clouds over the Amazon, *Science*, *321*, 946–949.

Kuhn, U., S. Rottenberger, T. Biesenthal, C. Ammann, A. Wolf, G. Schebeske, S. T. Oliva, T. M. Tavares, and J. Kesselmeier (2002), Exchange of short-chain monocarboxyclic organic acids by vegetation at a remote tropical forest site in Amazonia, *J. Geophys. Res.*, *107*(D20), 8069, doi:10.1029/2000JD000303.

Langenfelds, R. L., R. J. Francey, B. C. Pak, L. P. Steele, J. Lloyd, C. M. Trudinger, and C. E. Allison (2002), Interannual growth rate variations of atmospheric CO_2 and its $\delta^{13}C$, H_2, CH_4, and CO between 1992 and 1999 linked to biomass burning, *Global Biogeochem. Cycles*, *16*(3), 1048, doi:10.1029/2001GB001466.

Lanser, D., and J. G. Verwer (1998), Analysis of Operator Splitting for Advection-Diffusion-Reaction Problems from Air Pollution Modeling, CWI Report MAS-R9805.

Lavoué, D., C. Liousse, H. Cachier, B. J. Stocks, and J. G. Goldammer (2000), Modeling of carbonaceous particles emitted by boreal and temperate wildfires at northern latitudes, *J. Geophys. Res.*, *105***,** 26,871–26,890.

Lin, J. C., T. Matsui, R. A. Pielke Sr., and C. Kummerow (2006), Effects of biomass burning-derived aerosols on precipitation and clouds in the Amazon basin: a satellite-based empirical study, *J. Geophys. Res.*, *111*, D19204, doi:10.1029/2005JD006884.

Longo, K. M., A. M. Thompson, V. W. J. H. Kirchhoff, L. A. Remer, S. R. de Freitas, M. A. F. S. Dias, P. Artaxo, W. Hart, J. D. Spinhirne, and M. A. Yamasoe (1999), Correlation between smoke and tropospheric ozone concentration in Cuiabá during Smoke, Clouds, and Radiation-Brazil (SCAR-B), *J. Geophys. Res.*, *104*, 12,113–12,129.

Longo, K. M., S. R. Freitas, M. Silva Dias, and P. Silva Dias (2006), Numerical modeling of the biomass-burning aerosol direct radiative effects on the thermodynamics structure of the atmosphere and convective precipitation [CD-ROM], in *Proceedings of 8th International Conference on Southern Hemisphere Meteorology and Oceanography (ICSHMO), Foz do Iguaçu, Brasil*, pp. 283–289, INPE, São José dos Campos, ISBN 85-17-00023-4.

Longo, K. M., S. R. Freitas, A. Setzer, E. Prins, P. Artaxo, and M. O. Andreae (2007), The Coupled Aerosol and Tracer Transport model to the Brazilian developments on the Regional Atmospheric Modeling System. Part 2: Model sensitivity to the biomass burning inventories, *Atmos. Chem. Phys. Disc.*, *7*, 8571–8595.

Lyons, W. A., T. E. Nelson, E. R. Williams, J. A. Cramer, and T. R. Turner (1998), Enhanced positive cloud-to-ground lightning in thunderstorms ingesting smoke from fires, *Science*, *282*, 77–80.

Marengo, J. A., A. Cornejo, P. Satyamurty, C. A. Nobre, and W. Sea (1997a), Cold waves in the South American continent: The strong event of June 1994, *Mon. Weather Rev.*, *125*, 2759–2786.

Marengo, J. A., C. A. Nobre, and A. D. Culf (1997b), Climatic impacts of the "friagens" in the Amazon region, *J. Appl. Meteorol.*, *36*, 1553–1566.

Marengo J. A., C. A. Nobre, J. Tomasella, M. Oyama, G. Sampaio, H. Camargo, L. M. Alves, R. de Oliveira (2008), The drought of Amazonia in 2005, *J. Clim.*, *21*, 495–516.

Marengo, J., C. A. Nobre, R. A. Betts, P. M. Cox, G. Sampaio, and L. Salazar (2009), Global warming and climate change in Amazonia: Climate-vegetation feedback and impacts on water resources, *Geophys. Monogr. Ser*., doi:10.1029/2008GM000743, this volume.

Martins, J. A., M. A. F. Silva Dias, and F. L. T. Goncalves (2009), Impact of biomass burning aerosols on precipitation in the Amazon: A modeling case study, *J. Geophys. Res.*, *114*, D02207, doi:10.1029/2007JD009587.

Mason, S. A., R. J. Field, R. J. Yokelson, M. A. Kochivar, M. R. Tinsley, D. E. Ward, and W. M. Hao (2001), Complex effects arising in smoke plume simulations due to inclusion of direct emissions of oxygenated organic species from biomass combustion, *J. Geophys. Res.*, *106*(D12), 12,527–12,539.

Mason, S. A., J. Trentmann, T. Winterrath, R. J. Yokelson, T. J. Christian, L. J. Carlson, T. R. Warner, L. C. Wolfe, and M. O. Andreae (2006), Intercomparison of two box models of the chemical evolution in biomass-burning smoke plumes, *J. Atmos. Chem.*, *55*, 273–297, doi:10.1007/s10874-006-9039-5.

Mauzerall, D. L., J. A. Logan, D. J. Jacob, B. E. Anderson, D. R. Blake, J. D. Bradshaw, B. Heikes, G. W. Sachse, H. Singh, and B. Talbot (1998), Photochemistry in biomass burning plumes and implications for tropospheric ozone over the tropical South Atlantic, *J. Geophys. Res.*, *103*, 8401–8423.

McMillan, W. W., C. Barnet, L. Strow, M. T. Chahine, M. L. McCourt, J. X. Warner, P. C. Novelli, S. Korontzi, E. S. Maddy, and S. Datta (2005), Daily global maps of carbon monoxide from NASA's Atmospheric Infrared Sounder, *Geophys. Res. Lett.*, *32*, L11801, doi:10.1029/2004GL021821.

Morton, D. C., R. S. Defries, Y. E. Shimabukuro, O. L. Anderson, F. del B. Espírito Santo, M. Hansen, and M. Carroll (2005), Rapid assessment of annual deforestation in the Brazilian Amazon using MODIS data, *Earth Interact.*, *9*(8), EI139, doi:10.1175/EI139.1.

Morton, D. C., R. S. DeFries, Y. E. Shimabukuro, L. O. Anderson, E. Arai, F. Espirito-Santo, R. Freitas, and J. Morisette (2006), Cropland expansion changes deforestation dynamics in the southern Brazilian Amazon, *Proc. Natl. Acad. Sci. U. S. A.*, *103*(39), 14,637–14,641.

Nober, F. J., H.-F. Graf, and D. Rosenfeld (2003), Sensitivity of the global circulation to the suppression of precipitation by anthropogenic aerosols, *Global Planet. Change*, *37*, 57–80.

Nobre, C. A., P. J. Sellers, and J. Shukla (1991), Amazonian deforestation and regional climate change, *J. Clim.*, *4*, 957–988.

Nobre, C. A., G. O. Obregón, J. A. Marengo, R. Fu, and G. Poveda (2009), Characteristics of Amazonian climate: Main features, *Geophys. Monogr. Ser.*, doi:10.1029/2008GM000720, this volume.

Oliveira, P. H. F., P. Artaxo, C. Pires, S. De Lucca, A. Procopio, B. Holben, J. Schafer, L. F. Cardoso, S. C. Wofsy, and H. R. Rocha (2007), The effects of biomass burning aerosols and clouds on the CO_2 flux in Amazonia, *Tellus, Ser. B*, *59*, 338–349, doi:10.1111/j.1600-0889.2007.00270.x.

Olivier, J., A. Bouwman, J. Berdowski, J. Bloos, A. Visschedijk, C. van der Mass, and P. Zandveld, (1999), Sectoral emission inventories of greenhouse gases for 1990 on a per country basis as well as on 1 × 1 degrees, *Environ. Sci. Policy*, *2*, 241–263.

Pereira, G. (2008), O uso de satélites ambientais para a estimativa dos fluxos de gases traços e de aerossóis liberados na queima de biomassa e sua assimilação em modelos numéricos de qualidade do ar, Master thesis in Remote Sensing—Instituto Nacional de Pesquisas Espaciais (INPE), São José dos Campos, Brazil. (Available at http://urlib.net/sid.inpe.br/mtc-m17@80/2008/02.13.16.15).

Pickering, K. E., R. R. Dickerson, G. J. Huffman, J. F. Boatman, and A. Schanot (1988), Trace gas transport in the vicinity of frontal convective clouds, *J. Geophys. Res.*, *93*(D1), 759–773.

Prins, E. M., J. M. Feltz, W. P. Menzel, and D. E. Ward (1998), An overview of GOES-8 diurnal fire and smoke results for SCAR-B and 1995 fire season in South America, *J. Geophys. Res.*, *103*(D24), 31,821–31,835.

Procopio, A. S., L. A. Remer, P. Artaxo, Y. J. Kaufman, and B. N. Holben (2003), Modeled spectral optical properties for smoke aerosols in Amazonia, *Geophys. Res. Lett.*, *30*(24), 2265, doi:10.1029/2003GL018063.

Procopio, A. S., P. Artaxo, Y. J. Kaufman, L. A. Remer, J. S. Schafer, and B. N. Holben (2004), Multiyear analysis of amazonian biomass burning smoke radiative forcing of climate, *Geophys. Res. Lett.*, *31*, L03108, doi:10.1029/2003GL018646.

Radke, L. F., D. A. Hegg, P. V. Hobbs, J. D. Nance, J. H. Lyons, K. K. Laursen, R. E. Weiss, P. J. Riggan, and D. E. Ward (1991), Particulate and trace gas emissions from large biomass fires in North America, in *Global Biomass Burning*, edited by J. Levine, MIT Press, Cambridge, Mass.

Richardson, J. L., J. Fishman, and G. L. Gregory (1991), Ozone budget over the Amazon: Regional effects from biomass-burning emissions, *J. Geophys. Res.*, *96*, 13,073–13,087.

Riggan, P. J., R. G. Tissell, R. N. Lockwood, J. A. Brass, J. A. R. Pereira, H. S. Miranda, A. C. Miranda, T. Campos, and R. Higgins (2004), Remote measurement of energy and carbon flux from wildfires in Brazil, *Ecol. Appl.*, *14*, 855–872.

Rissler, J., A. Vestin, E. Swietlicki, G. Fisch, J. Zhou, P. Artaxo, and M. O. Andreae (2006), Size distribution and hygroscopic properties of aerosol particles from dry-season biomass burning in Amazonia, *Atmos. Chem. Phys.*, *6*, 471–491.

Roberts, G. C., A. Nenes, J. H. Seinfeld, and M. O. Andreae (2003), Impact of biomass burning on cloud properties in the Amazon Basin, *J. Geophys. Res.*, *108*(D2), 4062, doi:10.1029/2001JD000985.

Robock, A. (1991), Surface cooling due to forest fire smoke, *J. Geophys. Res.*, *96*, 20,869–20,878.

Rosenfeld, D., Y. J. Kaufman, and I. Koren (2006), Switching cloud cover and dynamical regimes from open to closed Benard cells in response to the suppression of precipitation by aerosols, *Atmos. Chem. Phys.*, *6*, 2503–2511.

Rosenfeld, D., U. Lohmann, G. B. Raga, C. D. O'Dowd, M. Kulmala, S. Fuzzi, A. Reissell, and M. O. Andreae (2008), Flood or drought: How do aerosols affect precipitation?, *Science*, *321*, 1309–1313.

Ross, J. L., P. V. Hobbs, and B. Holben (1998), Radiative characteristics of regional hazes dominated by smoke from biomass burning in Brazil: Closure tests and direct radiative forcing, *J. Geophys. Res.*, *103*, 31,925–31,941.

Rummel, U., C. Ammann, A. Gut, F. X. Meixner, and M. O. Andreae (2002), Eddy covariance measurements of nitric oxide flux within an Amazonian rain forest, *J. Geophys. Res.*, *107*(D20), 8050, doi:10.1029/2001JD000520.

Rummel, U., C. Ammann, G. A. Kirkman, M. A. L. Moura, T. Foken, M. O. Andreae, and F. X. Meixner (2007), Seasonal variation of ozone deposition to a tropical rainforest in southwest Amazonia, *Atmos. Chem. Phys.*, *7*, 5415–5435.

Satyamurty, P., C. Nobre, and P. Silva Dias (1998), South America, in *Meteorology of the Southern Hemisphere*, edited by D. Karoly and D. Vincent, *Meteorol. Monogr.*, *27*(49), 119–139.

Schafer, J. S., B. N. Holben, T. F. Eck, M. A. Yamasoe, and P. Artaxo (2002a), Atmospheric effects on insolation in the Brazilian Amazon: Observed modification of solar radiation by clouds and smoke and derived single scattering albedo of fire aerosols, *J. Geophys. Res.*, *107*(D20), 8074, doi:10.1029/2001JD000428.

Schafer, J. S., T. F. Eck, B. N. Holben, P. Artaxo, M. A. Yamasoe, and A. S. Procopio (2002b), Observed reductions of total solar irradiance by biomass-burning aerosols in the Brazilian Amazon and Zambian Savanna, *Geophys. Res. Lett.*, *29*(17), 1823, doi:10.1029/2001GL014309.

Schafer, J. S., T. F. Eck, B. N. Holben, P. Artaxo, and A. F. Duarte (2008), Characterization of the optical properties of atmospheric aerosols in Amazônia from long-term AERONET monitoring (1993–1995 and 1999–2006), *J. Geophys. Res.*, *113*, D04204, doi:10.1029/2007JD009319.

Schroeder, W., A. Alencar, E. Arima, and A. Setzer (2009), The spatial distribution and interannual variability of fire in Amazonia, *Geophys. Monogr. Ser.*, doi:10.1029/2008GM000724, this volume.

Seinfeld, J. H., and S. N. Pandis (1998), *Atmospheric Chemistry and Physics: From Air Pollution to Climate Change*, John Wiley, New York.

Setzer, A. W., and M. C. Pereira (1991), The Operational detection of fires in Brazil with NOAA-AVHRR, 24th International Symposium on Remote Sensing of the Environment, Rio de Janeiro, Brazil, pp. 76–77.

Setzer, A. W., and J. P. Malingreau (1996), AVHRR monitoring of vegetation fires in the tropics: Towards a global product, in *Biomass Burning and Global Change*, edited by J. Levine, pp. 25–39, MIT Press, Cambridge, Mass.

Silva Dias, M. A. F., et al. (2002), Cloud and rain processes in a biosphere-atmosphere interaction context in the Amazon Region, *J. Geophys. Res.*, *107*(D20), 8072, doi:10.1029/2001JD000335.

Smith, A. M. S., and M. J. Wooster (2005), Remote classification of head and backfire types from MODIS fire radiative power and smoke plume observations, *Int. J. Wildland Fire*, *14*, 249–254.

Stull, R. B. (1988), *An Introduction to Boundary Layer Meteorology*, Springer, Dordrecht.

Talbot, R. W., M. O. Andreae, T. W. Andreae, and R. C. Harriss (1988), Regional aerosol chemistry of the Amazon Basin during the dry season, *J. Geophys. Res.*, *93*, 1499–1508.

Thompson, A. M., et al. (1996), Ozone over southern Africa during SAFARI-92/TRACE A, *J. Geophys. Res.*, *101*, 23,793–23,807.

Thompson, A. M., J. C. Witte, R. D. Hudson, H. Guo, J. R. Herman, and M. Fujiwara (2001), Tropical tropospheric ozone and biomass burning, *Science*, *291*, 2128–2132.

Trentmann, J., R. J. Yokelson, P. V. Hobbs, T. Winterrath, T. J. Christian, M. O. Andreae, and S. A. Mason (2005), An analysis of the chemical processes in the smoke plume from a savanna fire, *J. Geophys. Res.*, *110*, D12301, doi:10.1029/2004JD005628.

Turquety, S., et al. (2007), Inventory of boreal fire emissions for North America in 2004: Importance of peat burning and pyroconvective injection, *J. Geophys. Res.*, *112*, D12S03, doi:10.1029/2006JD007281.

Van der Werf, G. R., J. T. Randerson, L. Giglio, G. J. Collatz, and P. S. Kasibhatla (2006), Interannual variability in global biomass burning emission from 1997 to 2004, *Atmos. Chem. Phys.*, *6*, 3423–3441.

Vera, C., et al. (2006), The South American Low-Level Jet Experiment, *Bull. Am. Meteorol. Soc.*, *87*(1), doi:10.1175/BAMS-87-1-63.

Vestin, A., J. Rissler, E. Swietlicki, G. Frank, and M. O. Andreae (2007), Cloud-nucleating properties of the Amazonian biomass burning aerosol: Cloud condensation nuclei measurements and modeling, *J. Geophys. Res.*, *112*, D14201, doi:10.1029/2006JD008104.

Wang, J., S. A. Christopher, U. S. Nair, J. S. Reid, E. M. Prins, J. Szykman, and J. L. Hand (2006), Mesoscale modeling of Central American smoke transport to the United States: 1. "Top-down" assessment of emission strength and diurnal variation impacts, *J. Geophys. Res.*, *111*, D05S17, doi:10.1029/2005JD006416.

Ward, D. E., R. A. Susott, J. B. Kauffman, R. E. Babbitt, D. L. Cummings, B. Dias, B. N. Holden, Y. J. Kaufman, R. A. Rasmussen, and A. W. Setzer (1992), Smoke and fire characteristics for Cerrado and deforestation burns in Brazil: BASE-B experiment, *J. Geophys. Res.*, *97*, 14,601–14,619.

Williams, E., et al. (2002), Contrasting convective regimes over the Amazon: Implications for cloud electrification, *J. Geophys. Res.*, *107*(D20), 8082, doi:10.1029/2001JD000380.

Yamasoe, M. A., C. von Randow, A. O. Manzi, J. S. Schafer, T. F. Eck, and B. N. Holben (2006), Effect of smoke and clouds on the transmissivity of photosynthetically active radiation inside the canopy, *Atmos. Chem. Phys.*, *6*, 1645–1656.

Yanenko, N. N. (1971), *The Method of Fractional Steps: The Solution of Problems of Mathematical Physics in Several Variables*, Springer, New York.

Yokelson, R. J., D. W. T. Griffith, and D. E. Ward (1996), Open-path Fourier transform infrared studies of large-scale laboratory biomass fires, *J. Geophys. Res.*, *101*(D15), 21,067–21,080.

Yokelson, R. J., R. Susott, D. E. Ward, J. Reardon, and D. W. T Griffith (1997), Emissions from smoldering combustion of biomass measured by open-path Fourier transform infrared spectroscopy, *J. Geophys. Res.*, *102*, 18,865–18,877.

Yokelson, R. J., I. T. Bertschi, T. J. Christian, P. V. Hobbs, D. E. Ward, and W. M. Hao (2003), Trace gas measurements in nascent, aged, and cloud-processed smoke from African savanna fires by airborne Fourier transform infrared spectroscopy (AFTIR), *J. Geophys. Res.*, *108*(D13), 8478, doi:10.1029/2002JD002322.

Yokelson, R. J., T. G. Karl, P. Artaxo, D. R. Blake, T. J. Christian, D. W. T. Griffith, A. Guenther, and W. M. Hao (2007), The tropical forest and fire emissions experiment: Overview and airborne fire emission factor measurements, *Atmos. Chem. Phys.*, *7*, 5175–5196.

Yokelson, R. J., T. J. Christian, T. G. Karl, and A. Guenther (2008), The tropical forest and fire emissions experiment: Laboratory fire

measurements and synthesis of campaign data, *Atmos. Chem. Phys.*, *8*, 3509–3527.

Yokelson, R., et al. (2009), Emissions from biomass burning in the Yucatan, in press, *Atmos. Chem. Phys. Disc.*, *9*, 767–835.

Zhang, Y., R. Fu, H. Yu, R. E. Dickinson, R. N. Juarez, M. Chin, and H. Wang (2008), A regional climate model study of how biomass burning aerosol impacts land-atmosphere interactions over the Amazon, *J. Geophys. Res.*, *113*, D14S15, doi:10.1029/2007JD009449.

M. O. Andreae, Max Planck Institute, P.O. Box 3060, D-55020 Mainz, Germany. (andreae@mpch-mainz.mpg.de)

P. Artaxo, Institute of Physics, University of São Paulo, Rua do Matao, Travessa R. 187, São Paulo, SP 05508-900, Brazil. (artaxo@if.usp.br)

S. R. Freitas, Center for Weather Forecast and Climate Studies, National Institute for Space Research, Rodovia Presidente Dutra, km 40, Cachoeira Paulista, SP 12630–000, Brazil. (saulo.freitas@cptec.inpe.br)

K. M. Longo, Center for Space and Atmospheric Sciences, National Institute for Space Research, Av. Dos Astronautas, 1758 Jardim da GranjaSão, José dos Campos, SP 12227-010, Brazil. (karla.longo@dge.inpe.br)

R. Yokelson, Department of Chemistry, University of Montana, Missoula, MT 59812, USA. (bob.yokelson@umontana.edu)